REPORT NO.
UCB/EERC-86/11
NOVEMBER 1987

EARTHQUAKE ENGINEERING RESEARCH CENTER

MECHANICAL CHARACTERISTICS OF BASE ISOLATION BEARINGS FOR A BRIDGE DECK MODEL TEST

by

JAMES M. KELLY
IAN G. BUCKLE
CHAN GHEE KOH

Report to the National Science Foundation

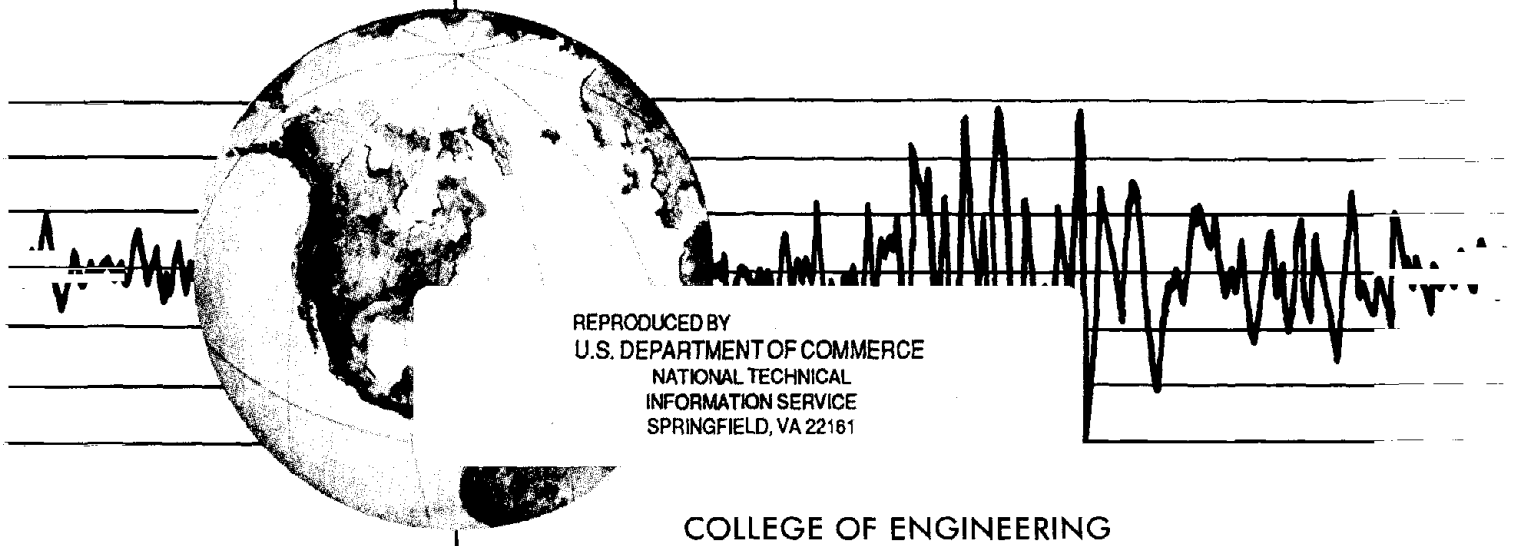

COLLEGE OF ENGINEERING

UNIVERSITY OF CALIFORNIA AT BERKELEY

For sale by the National Technical Information Service, U.S. Department of Commerce, Springfield, Virginia 22161

See back of report for up to date listing of EERC reports.

MECHANICAL CHARACTERISTICS OF BASE ISOLATION BEARINGS FOR A BRIDGE DECK MODEL TEST

by

Professor James M. Kelly
Department of Civil Engineering
University of California, Berkeley

Dr. Ian G. Buckle
Computech Engineering Services
Berkeley, California

Dr. Chan Ghee Koh
Department of Civil Engineering
University of California, Berkeley

A report on research sponsored by
the National Science Foundation
(Grant CEE-8213604)

Report No. UCB/EERC-86/11
Earthquake Engineering Research Center
College of Engineering
University of California, Berkeley

November 1987

ABSTRACT

This report describes the mechanical characteristics of rubber bearings designed for a base isolated bridge deck model which represents a typical highway bridge superstructure. Two different forms of isolation system were used in the test program. The first set of isolators were elastomeric bearings made from natural rubber layers and reinforced with steel plates. The second set of isolators were also elastomeric bearings of the same construction as the first set but with a lead plug on a vertical axis to enhance damping. To satisfy the dynamic similitude laws for the model, the bearings were unusually slender by current code specifications and outside the range of height-to-width ratios commonly accepted for stability of elastomeric bearings in the United States.

Static compression and shear tests, cyclic shear tests at different compression loads, and a series of shaking table tests were undertaken at the Earthquake Engineering Research Center of the University of California at Berkeley to establish fundamental stiffnesses, buckling loads and dynamic performance of the bearings. Of particular interest is the confirmation of theoretical predictions of the static stiffnesses, the buckling loads using a Southwell plot procedure, the reduction in lateral stiffness due to vertical load, and the limiting shear displacement defining the onset of overturning instability.

ACKNOWLEDGMENTS

The research described in this report was supported by the National Science Foundation, Grant No. CEE-8213604, through the Earthquake Hazards Mitigation Program under the direction of Dr. A. J. Eggenberger. The bearings were provided by Oil States Industries, Inc., Athens, Texas. The authors of this report are grateful for their support. The earthquake simulator study was performed while Dr. Buckle was on leave from the University of Auckland, New Zealand. This sabbatical, as well as special leave from the University of Auckland, is acknowledged.

TABLE OF CONTENTS

LIST OF TABLES

LIST OF FIGURES

1. INTRODUCTION

1.1 Background

Base isolation is a design strategy founded on the premise that a structure can be substantially decoupled from damaging horizontal components of earthquake motions so that levels of force and acceleration in the structure will be significantly reduced.

The principle of base isolation is to introduce flexibility at the base of a structure in the horizontal plane, while at the same time adding one or more damping elements to restrict the amplitude or extent of the motion caused by an earthquake. The essential design objective is to ensure that the period of the structure is well above that of the predominant earthquake input.

The concept of base isolating structures from the damaging effects of earthquakes is not new. The first patent for a base isolation scheme was taken out in 1907 and, since that time, several proposals with similar objectives have been made. Nevertheless, because of practical difficulties with the isolation schemes and their hardware, until very recently few structures had been designed and built using this concept.

Most isolation systems contain the following three basic elements:

(i) a flexible mounting so that the period of vibration of the total system is lengthened sufficiently to reduce the force response;

(ii) a damper or energy dissipator so that the relative deflections between building and ground can be controlled to a practical design level; and

(iii) a means of providing rigidity under low (service) load levels such as wind and minor earthquakes.

Mechanisms for introducing additional flexibility are numerous and include elastomeric pads, sliding plates, rollers, cable suspensions, sleeved piles and rocking (stepping) foundations. Of these the elastomeric bearing has received the greatest attention. This is because bridge structures have, for a number of years, been successfully

supported on elastomeric bearings to accommodate thermal and shrinkage effects. Numerous examples also exist where buildings have been successfully mounted on elastomeric pads. Over one hundred structures in Europe and Australia have been built on rubber bearings to isolate them from vertical vibrations generated by nearby subway and surface rail transit systems. All are performing well more than thirty years after construction.

The elastomeric bearing is particularly suitable for isolation applications because additional flexibility and period shift can be attained by increasing the thickness of the bearing. While the introduction of lateral flexibility is highly desirable, additional vertical flexibility is not. Vertical rigidity is maintained in an elastomeric bearing by sandwiching steel shims between each rubber layer. The steel shims, which are bonded to each layer of rubber, constrain lateral deformation of the rubber resulting in vertical stiffnesses several hundred times the lateral stiffness.

Thirty years of field experience with elastomeric bearings have shown them to be durable and reliable elements. Consequently, they are now being used for seismic isolation in several countries, including the United States of America. Although in most cases, the bearings are of the same general form as those used in conventional bridge design, there are a number of distinct differences between conventional (bridge) bearings and isolation bearings. A summary of these differences is followed by some discussion of them.

Compressive stresses are higher in isolation bearings, so that when designing for axial load, a rational method of design that includes the effect of high shear strain is required.

Isolation bearings are taller than bridge bearings and are therefore more slender. The buckling limit state needs careful evaluation.

During a maximum credible earthquake isolation bearings are expected to deform to much higher levels of shear strain than encountered in non-seismic

applications. Performance at high shear strain needs to be considered since change in height, reduction in footprint area and susceptibility to rollover all become significant with high shear strain.

Isolation bearings are sometimes structurally modified to accept a core or plug of material to enhance the damping characteristics. The effect of a hole on the shear and axial stiffness of a bearing needs to be determined.

Rated Load

The method of rating an elastomeric isolation bearing for axial load must be more rigorous than for a conventional bridge bearing because of the combination of high axial load and large shear strain. Limiting the compressive stress to an allowable value does not adequately account for the combination of strains resulting from large axial load and high shear strain. An alternative procedure is therefore required for the design of isolation bearings. Procedures have been adopted in several European and British codes in which the total shear strain in the elastomer, from all sources, is limited to a fraction of the ultimate elongation-at-break. If isolation bearings are designed to these more appropriate procedures (that is, a limited strain criterion), the resulting compressive stress is found to exceed the allowable limit in the U.S. code [1].

Slenderness

Elastomeric isolation bearings are more slender (taller) than those used for bridge expansion bearings and their height-to-width ratios approach or exceed current bridge code limits. These limitations are required to ensure stability of the bearing and predictable performance. They encourage bearing shapes which deform primarily in shear, rather than flexure, and as a result simplified design procedures can be used. For example, the AASHTO Specifications [1,2] for highway bridge bearings and the AREA Railway Bridge Specification [3] limit the total rubber thickness to less than one-third of the length or one-half of the width of the bearing (whichever is the

smaller) to ensure squat geometry. The British Specification BE 1/76 [4] places a restriction on both the individual layer thickness and the total rubber thickness. Both the British Standard BS 5400 (Part 9A: Code of Practice for Bearing Design) [5], and the UIC 772R Specification by the International Union of Railways [6] adopt a limitation based on compressive stress, shear modulus and shape factor. These various code requirements for slenderness are summarized in Table 1.

Stability

Shear strains greater than 50%, and sometimes as high as 150%, are to be expected in isolation bearings. The existence of these strains in combination with high axial load must be considered in design. The reduction in footprint leads to locally high compressive stresses and buckling loads are dramatically reduced in almost direct proportion to the loss in area. Overturning of the bearing, however, may occur before the onset of buckling and both limit states need careful assessment.

Other issues that need to be considered for elastomeric isolation bearings include the reduction in lateral stiffness with increasing vertical load and the reduction in height with increasing shear strain.

1.2 Scope of the Report

Slender elastomeric bearings were recently designed and fabricated for a research project on the performance of base isolated bridge superstructures at the Earthquake Engineering Research Center of the University of California at Berkeley [7]. Since the model superstructure was relatively light, the bearings were correspondingly higher than normal in order to give a mass-to-stiffness ratio that ensured a fundamental period of about 1.5 seconds. The bearings that were designed and tested during this project had an overall height-to-width ratio of almost unity. Since these bearings did not meet the requirements of the AASHTO and AREA codes and were close to the limits of other codes, the opportunity was taken to make a careful examination of

their mechanical properties (static and dynamic stiffnesses, buckling load, overturning displacement, etc.) and to compare these properties with theoretical predictions for slender bearings.

Many of the issues indicated above were studied using the results of single component testing and of shaking table testing. This report describes the results of these tests as they affect the design of elastomeric isolation bearings. Correlation with theoretical prediction is made wherever possible and several new theories are postulated for elastomeric bearing performance.

2. BEARING DESIGN AND MATERIAL SPECIFICATIONS

2.1 Base Isolated Bridge Deck Model

The bearings were designed to support a model bridge deck for the purpose of studying seismic isolation of a bridge superstructure using the 20 ft x 20 ft shaking table of the Earthquake Simulator Laboratory. The model deck comprised two parallel, 20 ft long, WF16 steel girders spaced 6 ft apart and connected transversely by channel sections and angle cross-bracing (Figures 1 and 2). These girders supported precast concrete slabs and lead ballast to give a total weight of 96 kips, typical of short-span reinforced concrete decks.

The isolation bearings were designed to give an effective period to the deck of 1.5 seconds so that real time unscaled records of ground motion could be used for table input motions. In this sense the model scale factor was unity, but because of the physical dimensions of the table, the model was limited in size, if not in weight, and a length scale factor of 4 was used for geometry. However, since the vibration modes of particular interest were predominantly in the horizontal plane, this length scale factor was not important — the deck being assumed to be rigid in its own plane.

2.2 Material Properties and Bearing Design Parameters

The formulation from which the bearings were made was developed by the Malaysian Rubber Producers' Research Association (MRPRA). To develop the frequency characteristics for the bridge deck, it was necessary to select a fairly soft rubber and that chosen was MRPRA EDS 39 [8] with a nominal shear modulus (G) at 50% strain of 100 psi and an IRHD of 55. The rubber as compounded by the manufacturer had a hardness of 50 and a 50% shear modulus of 103 psi and a minimum elongation-at-break of 550%. The elastic modulus (E) at 50% strain was 412 psi.

The bearings were manufactured by Oil States Industries Inc., Athens, Texas. They were all 8-1/2 inches square in plan and 7-7/8 inches in overall height (Figure 3). Fourteen natural rubber layers, each 3/8 inch thick were used to obtain the desired rubber thickness of 5-1/4 inches. A central hole, 1-1/2 inches in diameter, was formed in each bearing and a lead cylinder pressed into this hole after tests on the plain, unfilled bearings were completed. The design earthquake for the bearings was El Centro 1940, 0.33g peak ground acceleration.

The shape factor of a 3/8-inch rubber layer including allowance for an unfilled 1-1/2 inch diameter hole is $S = 4.52$. An estimate of the compression modulus is given by the standard formula [9]

$$E_c = E\,(1 + 2\kappa S^2) \tag{2.1}$$

where κ is 0.64 for MRPRA EDS 39 rubber. Thus $E_c = 11.2$ ksi.

Let A be the cross-sectional area of the bearing and T_r the total thickness of rubber layers in the bearing. The nominal shear stiffness given by

$$K_h = GA\,/\,T_r \tag{2.2}$$

is predicted to be 1.22 kips/in. and the axial stiffness given by

$$K_v = E_c A\,/\,T_r \tag{2.3}$$

is 132.6 kips/in.

Based on Haringx's theory [9,10,11], the critical (buckling) load is

$$P_{cr} = R\left[(1 + 4P_E/R)^{\frac{1}{2}} - 1\right]/2\,, \tag{2.4}$$

where

$P_E = \pi^2 T/H$
$R = K_r H$
$T = E_b\, I\, H/T_r$
I = moment of inertia of bearing about axis of bending
H = height of bearing excluding top and bottom plates
$E_b = E\,(1 + 0.742S^2)$ for a square bearing [12].

Thus the predicted buckling load of the rubber bearing without lead plug is 68.2

kips. The reduced shear stiffness at 25-kip axial load is given by

$$K_r = \frac{P}{H}\left[(1+\frac{P}{R})(\frac{\tan\beta}{\beta}-1)\right]^{-1} \qquad (2.5)$$
$$= 1.01 \text{kips/inch}$$

where

$$\beta = qH/2$$
$$q = [P\,(1+P/R\,)/\,T\,]^{1/2}$$
$$P = \text{axial load.}$$

In design codes, an important parameter affecting bearing stability is the ratio T_r/B, where B is the width of the bearing. For the given geometry this ratio is 0.62 which exceeds the AASHTO limit (Table 1) of 0.33 by a wide margin. However, since the rubber layer thickness t_r equals $0.04B$, the given bearing satisfies the BE 1/76 limitations (Table 1: $t_r \leq 0.25B$ and $T_r \leq B$) and the BS5440 and UIC 772R criteria which for the given geometry require that $T_r \leq 0.8B$ (Table 1: $G =$ 103 psi, $S = 4.52$, $\sigma_c =$ 390 psi). The limiting displacement to prevent overturning instability is discussed in Chapter 5.

3. STATIC TESTS OF BEARINGS AND SOUTHWELL PLOTS

3.1 Axial Stiffness (K_v)

Single bearings were tested in direct compression and a typical load-deflection curve is shown in Figure 4. Hysteresis is evident and the nonlinearity implies a variation with strain amplitude and load path. A mean value for stiffness may be computed by taking the slope of the line joining the origin to the point of load reversal. The value so obtained is 135 kips/inch which is in good agreement with the theoretical value (132.6 kips/inch) predicted for these bearings.

While slenderness does not appear to influence the axial stiffness, it was found necessary to include the surface area of the unfilled central hole in the calculation for shape factor which is then used to predict the axial stiffness.

3.2 Reduced Shear Stiffness (K_r)

Two bearings, separated by a steel plate, were placed in series in a compression test machine. An axial load of 25 kips was applied to both bearings and the steel plate pulled laterally to deform the bearings in shear. A plot of the shear force against the corresponding shear displacement is given in Figure 5.

The nonlinear nature of the bearing is again obvious and its hysteretic response is evident from the difference between the loading and unloading paths. The mean slope (from origin to point of load reversal) is 2.0 kips/inch, which implies an average shear stiffness for each bearing over this range (almost 80%) of 1.00 kip/inch. The tangential stiffness at 50% shear strain on the loading curve is 0.94 kip/inch per bearing. Both values are in good agreement with the predicted value of 1.01 kips/inch.

3.3 Buckling Load (P_{cr})

A Southwell plot [13,14] procedure was used to determine experimentally the buckling loads for the bearings. To simulate the field end support conditions (i.e. one end fixed against rotation and translation, the other fixed against rotation but free to translate freely), two bearings were again mounted in series in a compression test machine. However on this occasion they were separated from the steel platens of the compression machine and each other by wedge-shaped steel plates. These plates had been machined so that their load bearing surfaces were 1 degree out of parallel to each other and then oriented so as to introduce a small but finite eccentricity (δ_o) into the bearing "column". Figure 6 shows the general arrangement before axial compression was applied to the bearings.

Measurements of the axial load (P) and the corresponding horizontal deflection (δ) of the center wedge plate were recorded up to a maximum of 40 kips. Plots of δ/P against δ are shown in Figure 7 from which the Southwell procedure gives the critical load from the inverse of the slope of the line and the initial eccentricity from the intercept on the δ-axis. It is seen that the buckling load and eccentricity are 71.6 kips and 0.53 inch, respectively.

Alternatively, P may be plotted against P/δ (the so-called *reversed* Southwell plot) which is thought to give slightly more accurate estimates of critical load. This plot, from which the critical load is the intercept on the P-axis and the eccentricity the intercept on the P/δ-axis, is shown in Figure 8. The values for the buckling load and eccentricity are then 70.0 kips and 0.56 inch, respectively. The buckling load is in excellent agreement with the predicted 68.2 kips and confirms the adequacy of the Haringx formulation. The design load was 24 kips and therefore the factor of safety against buckling for these slender bearings was almost 3.

The theoretical initial eccentricity is 0.14 inch (Figure 6) but since no particular care was taken to align the bearings directly over one another when setting up the experiment, the actual eccentricity could have been much larger and a value of the order of 0.5 inch is not unreasonable.

4. CYCLIC SHEAR TESTS OF BEARINGS UNDER DIFFERENT COMPRESSION LOADS

4.1 Test Setup

A test rig was designed to subject a single bearing to combined static vertical and cyclic lateral loads. It consists of two heavily-braced reaction frames supporting a horizontal hydraulic actuator and two vertical actuators (Figure 9). The horizontal actuator can move sinusoidally according to the command signal from a controller. The vertical actuators apply, through a beam, a compression load to the bearing to simulate the gravity load effect. The vertical actuators are controlled electronically such that the total compression load is maintained at a specified constant load while the differential displacement between the actuators is always zero.

A force transducer is placed under the bearing specimen to measure the shear force and bending moment. A reaction block composed of a concrete base and a wide flange steel beam provides anchorage to the test floor. A rigid spacer is placed between the transducer and the bottom beam to maximize the length of the vertical actuators so that the change of vertical load component in the actuators due to lateral displacements becomes insignificant. Two struts connected perpendicular to the top beam enhance the transverse stability of the test rig.

The bearing specimens were subjected to a sinusoidal horizontal displacement under a constant compression load (P). Since the dynamic properties of rubber depend on the amplitude of motion, several series of tests were conducted at different displacement amplitudes. For each series of test results, the rubber properties were determined independently. The diagonal stiffness (K_d) of a hysteresis loop and the loss angle (ϕ) are determined, respectively, from

$$K_d = \frac{f_o}{d_o} \tag{4.1}$$

$$\phi = \sin^{-1}\left[\frac{A_{loop}}{\pi f_o\, d_o}\right] \tag{4.2}$$

where f_o and d_o are the amplitudes of the horizontal force and displacement, respectively, and A_{loop} is the area of the hysteresis loop per cycle. Each test is also used to determine the change in bearing height,

$$\Delta h_{\max} = \text{maximum } \Delta h(t) - \text{minimum } \Delta h(t) \tag{4.3}$$

In this calculation, correction is made to account for the horizontal displacement (the "arc" effect) and also the change in bearing height due to slight variation in the actual compression load.

4.2 Analytical Model and Parameter Identification

A viscoelastic $P-\Delta$ model, which takes into account significant shear deformation, is used here. This model is consistent with Haringx's theory but only considers the first mode; it is therefore called the "first-mode consistent model" [15]. For a homogeneous element, the complex shear stiffness can be shown to be

$$K_r^* \approx \frac{G^* A}{H}\left[1 + \frac{8}{\pi^2}\frac{(1+p^*)^2}{p_e - p^*(1+p^*)}\right]^{-1} \tag{4.4}$$

where

$$p_e = P_E / GA$$
$$p^* = \frac{P}{G^* A}$$
$$G^* = G(1 + i\,\gamma)$$

in which γ is the loss angle of the material. The dynamic shear stiffness and the loss angle of the bearing are, respectively,

$$K_d = |K_r^*| \tag{4.5}$$

$$\phi = \tan^{-1}\left(\frac{\text{Im}(K_r^*)}{\text{Re}(K_r^*)}\right). \tag{4.6}$$

Another quantity of interest is the height reduction of the bearing during the lateral motion. The height reduction of the bearing corresponding to a cyclic lateral force of $F(t) = f_o \cos(\omega t)$ is

$$\Delta h_{\max}(t) = \frac{H}{2} \mathrm{Re}\left[\frac{4}{\pi} \frac{f^*}{G^* A} + (0.5+p^*)\psi^* \right] \mathrm{Re}(\psi^*) \tag{4.7}$$

where

$$f^* = f_o \exp(i\omega t)$$
$$\psi^* = \frac{4}{\pi} \frac{f^*}{G^* A} \frac{(1+p^*)}{p_e - p^*(1+p^*)} .$$

The controlling parameters for the analytical model can be grouped as follows:

(i) H, the combined height of the rubber layers and steel plates (not including the top and bottom end plates).

(ii) γ, the material loss angle.

(iii) $(GA)_{eff}$, the effective GA of the bearing.

$$(GA)_{eff} = GA\ H/T_r \tag{4.8}$$

where T_r is the total thickness of all rubber layers. The scaling factor H/T_r is to account for the presence of the steel plates which are assumed to be rigid compared with rubber. This is done so that the bearing can be treated as if it were made of homogeneous material.

(iv) $(EI)_{eff}$, the effective EI of the bearing. If incompressibility is assumed for rubber and also a high shape factor, it can be shown (see Section 4.3 in reference 15), that

$$(EI)_{eff} \approx 2.23\, S^2 r^2 (GA)_{eff} \tag{4.9}$$

for a square-shaped bearing, where $r^2 = I/A$.

For the bearing with a central hole but containing no lead plug, the equivalent square bearing that has the same cross-sectional area and shape factor is used. Since H is known and $(EI)_{eff}$ is related to $(GA)_{eff}$, only two parameters (G and γ) are needed to define the bearing stiffness and damping characteristics for a fixed amplitude of motion. Although data sheets for rubber are available [8], the rubber used in the bearing may have somewhat different properties from the rubber used in the tests pertaining to the data sheets. It has also been observed in past experiments that the bearings usually have a higher damping factor than the smaller rubber specimens used in tests to obtain the data sheets; but the reason is not fully understood. Furthermore, different curing conditions affect the shear modulus of rubber. For these practical reasons, G and γ are estimated from tests of the actual bearing specimens, as follows:

(i) The value of γ is estimated from the initial portion of the damping curve since theoretically $\phi = \gamma$ at $P = 0$.

(ii) The value of G is similarly estimated from

$$K_d \approx (1+\tan^2\gamma)^{1/2}\left[\frac{H}{(GA)_{eff}}+\frac{H^3}{12(EI)_{eff}}\right]^{-1} \quad \text{at} \quad P \approx 0. \qquad (4.10)$$

Since there are inevitably some experimental errors in obtaining data for the initial flat portion of the curve, some slight adjustments in these two parameters are sometimes necessary to achieve a better correlation.

4.3 Bearings Without Lead Plug

The test data are summarized in Table 2. Using the foregoing parameter identification procedure, the loss factors of rubber for 1 inch, 3 inch and 5 inch shear tests are estimated to be 7%, 8% and 9%, respectively. The corresponding shear moduli are found to be 138 psi, 119 psi and 105 psi. In Figure 10 the

theoretical curves for K_d based on the first-mode consistent model are compared with the experimental data. It can be seen that the model gives a very good quantitative representation of the dynamic shear stiffness of the rubber bearing. Similar comparisons for the damping factor of the bearing are made in Figure 11. The quadratic variation of the damping factor of the bearing is clearly demonstrated by the experimental data and well described by the proposed model.

The experimental results for the height reduction of 1 inch tests were too small to be reliable. Only the results for 3 inch and 5 inch tests were considered. As shown in Figure 12, the scatter of the data points even for the same loading condition reveals the difficulty of measuring small $\Delta h_{\max}$. Considering the measurement problem, the test results of $\Delta h_{\max}$ agree satisfactorily with the first-mode consistent model.

The height reduction versus the horizontal displacement for the experiment and the theory are plotted for a full cycle in Figure 13. It is interesting to note that the "inward" and "outward" curves do not coincide but rather, form a loop. This happened in the tests. This phenomenon is not only due to the viscoelasticity of the material but is also a result of the significant shear deformation which is out of phase with the flexural deformation. Even with viscoelasticity taken into consideration, a regular column (i.e. neglecting shear deformation) fails to reproduce this phenomenon.

It is, however, very difficult to achieve a perfectly symmetric condition in the experimental setup and therefore the experimental curve is typically not quite symmetric. The solid curve in Figure 13 is an example from one of the actual tests, corrected for the changes in vertical displacement due to the arc effect and due to the slight variation of actual compression load. For clarity in comparison,

the theoretical curve in Figure 13 has been shifted up by 0.1 inch. It can be seen that the agreement between the theoretical loop and the experimental loop is good, except for the asymmetry of the latter. The non-symmetric behavior is believed to contribute partly to the discrepancies between the analytical and the experimental results for height reduction.

4.4 Bearings With Lead Plug

The bearing with a lead plug is also treated as if it were homogeneous. The parameters determined therefore represent some equivalent values for the rubber-lead composite bearing. Initially, the consistent model is used as a basic model rather than resorting to a more elaborate model that would take into account the elasto-plastic behavior of the lead plug.

Because of the presence of the lead plug the shear characteristics of the bearing are not related to the compression and bending behavior, therefore $(EI)_{eff}$ is taken to be independent of $(GA)_{eff}$. The test data are summarized in Table 3. With γ estimated to be 0.19, the best-fit values of $(GA)_{eff}$ and $(EI)_{eff}$ are found to be 10.7 kips and 2269 kip–in^2, respectively. Figures 14 and 15 show the good agreement between the experimental results for K_d and $\sin\phi$, respectively, and the first-mode consistent model. It is interesting to note that the damping factor of the bearing went as high as 96% (when P was close to the critical load). In Figure 16, the agreement for the height reduction is somewhat less satisfactory, especially near the buckling load.

5. OVERTURNING BEHAVIOR OF BEARINGS

5.1 Overturning Instability

An undesirable consequence of more slender bearings is their susceptibility to overturning. This is particularly important when elastomeric bearings are subject to high shear strains as may be the case during extreme earthquake events. Since typical mounting details are specifically designed to release tension from the bearing, overturing cannot be actively resisted by the support. Instead the bearing is restrained from rolling off its seating pad by the axial force couple which provides a restoring moment to the bearing. Premature overturning can therefore be prevented by increasing either the axial load or the bearing width or both, so as to increase the moment arm constituting the force couple. At the same time, the bearing height should be minimized so as to reduce, if possible, the overturning moment due to shear force. Combining both recommendations leads to a preference for squat geometry.

Figure 17 shows a bearing deformed laterally through a displacement Δ by a shear force (V) while carrying an axial load (P). If overturning is imminent, the axial forces are assumed to act at the extreme edges of the upper and lower shims or dowel plates. Equilibrium then requires:

$$V H = P (B - \Delta) \tag{5.1}$$

where H and B are the height of the bearing not including the two end plates and the width of the bearing, respectively. Now if the bearing is linear,

$$V = K_r \Delta \tag{5.2}$$

and it follows that the critical displacement Δ_c is given by

$$\Delta_c = PB / (P + K_r H) . \tag{5.3}$$

On the other hand, if the bearing is bilinear,

$$V = Q_d + K_r \Delta \tag{5.4}$$

where Q_d is defined in Figure 18; and then

$$\Delta_c = \frac{PB - Q_d H}{P + K_r H} . \tag{5.5}$$

Equations 5.1, 5.2 and 5.4 are illustrated in Figure 18. The intersection of Eqs. 5.1 and 5.2 gives the solution of Δ_c as defined in Eq. 5.3. Similarly the intersection of Eqs. 5.1 and 5.4 gives Δ_c as defined in Eq. 5.5. Overturning does not begin until Δ_c is exceeded, up to which point the bearing can be said to be unconditionally stable against overturning. However for equilibrium to be satisfied beyond this deflection, the shear force V must be reduced. The bearing stiffness appears to soften for it now has a negative tangential stiffness of $-P/H$. The secant stiffness is nevertheless still positive, but it is less than K_r. At this point the bearing is conditionally stable since its stability is dependent upon a reduction in shear force. If the bearing is being driven by a force-controlled mechanism and the force is not reduced, the bearing will overturn. Under random dynamic loads, such as those imposed during an earthquake, it is conceivable that a force reduction may occur at the required time and the bearing may follow the stable branch of the response curve to recover its original state without distress to itself or the supported structure.

Overturning does not physically occur until the deflection exceeds the width of the bearing and even then it may be prevented if the shear force should reverse in direction, as is again possible in some dynamic loading situations.

The importance of slenderness is also illustrated in Figure 18. If the height to width ratio (H/B) is taken as a measure of slenderness, it is seen that as the slenderness increases, the critical displacement Δ_c, which determines the onset of shear stiffness of the bearings, becomes smaller. It is also seen that the higher the shear stiffness of the bearings the smaller is Δ_c, a fact which gives rise to the reduced value for Δ_c for bilinear bearings of the same K_r.

5.2 Earthquake Simulator Tests

Shaking table tests were used here to study the overturning behavior of the bearings. The weight of the model bridge deck generates a constant axial load. By progressively increasing the intensity of table motion, it was also possible to initiate simultaneous overturning (rollout) of all four bearings supporting the bridge deck.

Based on Eq. 5.3, the critical displacement which defines the onset of rollout is found to be 6.26 inches for bearings without lead plugs. The beginning of instability should thus be evident in hysteresis loops that extend beyond 6 inches. Figure 19 shows one such loop for a plain bearing during loading by an ATC-3 spectrum compatible record which had been scaled to a peak table acceleration of 0.32g. Clearly, one cycle has driven the bearing beyond the limiting displacement and the bearing was then potentially unstable. However, a coincidental reduction in superstructure inertial forces has produced the shear force in the bearing at the same time, such that equilibrium and stability are both maintained. It is seen in Figure 19 that a peak displacement of 7.42 inches was produced before the motion reversed and the bearing recovered to its stable state.

Figure 20 shows the same bearing under a more severe ground motion (El Centro, peak acceleration scaled to 0.94g) in which the bearing did not recover and overturning occurred at 8.25-inch displacement (which is almost the overall width of the bearing). Collapse of the deck followed immediately. The agreement between the theoretical critical displacement and that shown in Figures 19 and 20 is excellent and confirms the validity of the overturning model. As shown in Figure 20, the intersection of the line $K_r \approx 1$ kip/in. and the line representing the slope of the decreasing branch gives $\Delta_c = 6.5$ inches which is in good agreement with the previously predicted value of 6.26 inches.

Further confirmation is possible by comparing the slope of the decreasing branch of the load deflection curve in Figure 20 against the theoretical value of $-P/H$. Experimentally this value is -3.77 kips/in. Taking P at 24 kips and H at 6.875 inches, the theoretical slope is -3.49 kips/in.

It is of interest to note that after collapse the bearings themselves showed no signs of failure despite imposed shear strains of 152%. No evidence of elastomer tearing, bond failure or permanent distortion was found. In fact, the collapsed bridge model was lifted and the same bearings reinstated for additional "rollout" tests with other earthquake records.

As noted in Chapter 2, these bearings were designed for the El Centro, 0.33g peak acceleration earthquake. The margin of safety against rollout was therefore almost 3, despite the slender nature of the bearings. The overturning experiments were repeated with the central hole in the bearings filled with lead. Since the lead cores dampen the response and reduce bearing displacements for the same earthquake intensity, a higher level of shaking can be tolerated before the overturning displacements are reached. It was found necessary to increase the table motion intensity by an additional factor of 1.74 to initiate the rollout of these bearings which implies a factor of safety against overturning of about 5.0.

It should be noted that the bridge model was totally free to translate sideways. In practice, abutment walls of side stops can be positioned to prevent excessive displacements (and perhaps overturning) occurring under extreme earthquake events.

6. CONCLUSIONS

Elastomeric bearings which are used as seismic isolation bearings are more slender than conventional elastomeric bearings. This report has discussed the implications of slenderness on their mechanical properties. The following conclusions are made:

(1) The vertical (axial) stiffness of a slender bearing is not influenced by slenderness and may be adequately predicted by conventional theory. However, for a bearing with a circular hole on its vertical axis, the shape factor should include the presence of the hole. First, only the bonded area of rubber should be used which is calculated from the dimensions of the shim plates less the area of the hole. Second, the area free to expand (bulge) should include the area facing into the hole. If, however, the hole is filled with say a lead core, this additional area term should not be used.

(2) The lateral (shear) stiffness of a slender bearing is strongly influenced by the vertical (axial) load -- an effect which is routinely ignored for squat bearings. For the test bearings with $T_r = 0.62\,L$, a 17% reduction in static lateral stiffness was found due to a vertical load equal to 35% of the critical load. This observation is in good agreement with the theoretical prediction by the Haringx theory.

(3) The first-mode consistent model developed to account for the $P-\Delta$ effect in the dynamic analysis of bearings is found to be appropriate. This analytical model is able to model the reduction of dynamic lateral stiffness and the increase in energy dissipation with increasing axial load. Both phenomena were observed in the experiments.

(4) The critical (buckling) load is conservatively given by the Gent/Haringx formulation. It may be confirmed experimentally without risk of failure or damage to the bearings, by use of Southwell's procedure. The factor of safety

against buckling for the test bearings was almost 3.

(5) The overturning displacements may be accurately predicted assuming that the axial forces which comprise the restoring couple act at the extreme edges of the upper and lower faces of the bearing. The experimental confirmation of these theoretical values was made during seismic excitation of a model bridge deck on the shaking table. The test bearings were designed for a peak ground acceleration of 0.33g. Rollout for an unfilled bearing occurred at 0.94g and for a lead-filled bearing at 1.6g. The factor of safety against rollout (overturning) was therefore in the range 3-5.

(6) The test bearings did not satisfy the present AASHTO requirements on slenderness. Nevertheless, the factors of safety against buckling and overturning were adequate (3 and higher). These observations, which have been made both experimentally and theoretically, appear to support the more relaxed limits used in foreign codes (BE 1/76, BS5400 and UIC 772R).

(7) Despite their slender proportion, the test bearings performed in a predictable and reliable manner with adequate factors of safety against collapse. The use of more refined theories such as those presented in this report for estimation of the mechanical properties of slender elastomeric bearings is recommended.

REFERENCES

1. *Standard Specifications for Highway Bridges, AASHTO, 13th edition*, Washington D. C., 1983.
2. *Standard Specifications for Laminated Elastomeric Bridge Bearings, AASHTO Specification for Materials M 251-74*, Washington D. C., 1974.
3. *Manual of Engineering Recommended Practice*, American Railway Engineering Association, 1988.
4. "Design Requirements for Elastomeric Bridge Bearings," *Technical Memorandum BE 1/76*, Highways Directorate, Department of Environment, Great Britain, 1976.
5. *British Standard BS5400: Steel, Concrete and Composite Bridges: Part 9A: Code of Practice for Design of Bearings*, British Standards Institution, Document 81/10/84, 1981.
6. "Code for the Use of Rubber Bearings for Rail Bridges," *UIC Code 772R*, International Union of Railways, Ways and Works Committee VII, Brussels, 1973.
7. J. M. Kelly, I. G. Buckle, and Hsiang-Chuan Tsai, "Earthquake Simulator Testing of a Base-Isolated Bridge Deck," *Report No. UCB/EERC-85/09*, University of California, Berkeley, 1985.
8. *Malaysian Rubber Producers' Research Association, Engineering Data Sheets, EDS 39*, Tun Abdul Razak Laboratory, Brickendonbury, Hertford, England, 1981.
9. A. N. Gent, "Elastic Stability of Rubber Compression Springs," *Journal of Mechanical Engineering Science*, 6(4): 318-326, 1964.
10. J. A. Haringx, "On Highly Compressive Helical Springs and Rubber Rods and their Applications to Free Mountings -- Parts I, II and III," *Philips Research Reports*, 1948-1949.
11. D. J. Derham and R. A. Waller, "Luxury Without Rumble," *The Consulting Engineer*, 39: 49, 1975.
12. A. N. Gent and E. A. Meinecke, "Compression, Bending, and Shear of Bonded Rubber Blocks," *Polymer Engineering and Science*, 10(1): 48-53, Jan. 1970.
13. R. V. Southwell, *An Introduction to the Theory of Elasticity for Engineers and Physicists*, Oxford University Press, 1936.

14. R. T. Marshall and H. M. Nelson, *Structures*, Pitmans, London, 1969.

15. C. G. Koh and J. M. Kelly, "Effects of Axial Load on Elastomeric Isolation Bearings," *Report No. UCB/EERC-86/12*, University of California, Berkeley, 1987.

TABLE 1

Code Limitations on Slenderness

Code	Limitation on T_r for Stability
AASHTO and AREA	$T_r \leq L / 3$ and $T_r \leq B / 2$
BE 1/76	$t_r \leq L / 4$ and $T_r \leq L$
BS5400 and UIC772R	$T_r \leq 2 L G S / 3 \sigma_c$

Notations: T_r : total rubber thickness

t_r : typical rubber layer thickness

L and B : length and width of bearing

G : shear modulus

S : shape factor

σ_c : compressive stress in bearing

TABLE 2

Cyclic Loading Test Results for Bearing Without Lead

d_0 (in.)	P (kips)	K_d (kips/in.)	$\sin\phi$ (%)	Δh_{max} (in.)
1	4.9	1.448	8.04	*
	9.9	1.360	8.61	*
	10.5	1.373	8.92	*
	19.8	1.150	10.38	*
	20.0	1.145	10.13	*
	20.0	1.143	10.14	*
	29.9	0.939	13.10	*
	30.0	0.999	12.59	*
	30.3	0.988	13.29	*
	30.1	0.958	12.90	*
	35.0	0.921	13.63	*
	35.0	0.856	15.53	*
	39.8	0.797	17.45	*
	45.5	0.734	20.61	*
	45.4	0.622	23.69	*
	50.3	0.542	28.57	*
	55.3	0.484	34.75	*
3	4.9	1.149	8.39	0.059
	9.8	1.104	8.46	0.064
	10.0	1.171	7.87	N.A.
	10.5	1.117	8.77	0.058
	19.8	0.968	9.40	0.077
	20.1	0.984	9.63	0.064
	29.9	0.746	15.15	0.087

Continued on Next Page.

TABLE 2 (Continued)

d_0 (in.)	P (kips)	K_d (kips/in.)	$\sin\phi$ (%)	Δh_{max} (in.)
3	30.0	0.812	14.24	0.068
	30.2	0.787	12.90	0.083
	34.5	0.702	17.69	0.070
	35.0	0.667	18.17	0.088
	39.7	0.569	24.10	0.094
	45.5	0.432	35.23	0.110
	50.3	0.278	65.79	0.128
5	9.7	0.929	10.22	0.143
	10.3	0.943	9.63	0.141
	19.9	0.861	13.14	0.185
	20.5	0.816	13.17	0.210
	20.5	0.797	13.21	0.274
	20.3	0.793	13.20	0.226
	20.7	0.785	13.39	0.235
	29.9	0.675	20.30	0.220
	30.1	0.605	19.96	0.261
	32.6	0.618	24.35	0.236
	35.4	0.480	29.23	0.280
	40.2	0.380	41.62	0.287
	45.5	0.270	68.22	0.304
	45.8	0.262	72.74	0.317

Notes: * Measurement of height reduction too small to be accurate.

N.A. Data not available because of instrument problem.

TABLE 3

Cyclic Loading Test Results for Bearing With Lead

d_0 (in.)	P (kips)	K_d (kips/in.)	$\sin\phi$ (%)	Δh_{max} (in.)
5	10	1.227	16.00	0.269*
	19.9	1.281	18.77	0.164
	29.6	1.122	26.18	0.202
	35.2	1.042	32.07	0.231
	40.2	0.934	39.30	0.255
	45.3	0.791	48.82	0.282
	19.6	1.296	22.32	0.172
	45.0	0.868	44.53	0.262
	50.3	0.694	60.55	0.266
	55.2	0.605	72.50	0.284
	59.9	0.527	91.15	0.300
	65.4	0.543	96.13	0.322

Notes:

(1) * indicates that partial roll-over was observed and data disregarded.

(2) The first 6 tests were done sequentially in one day and the last 6 tests three days later.

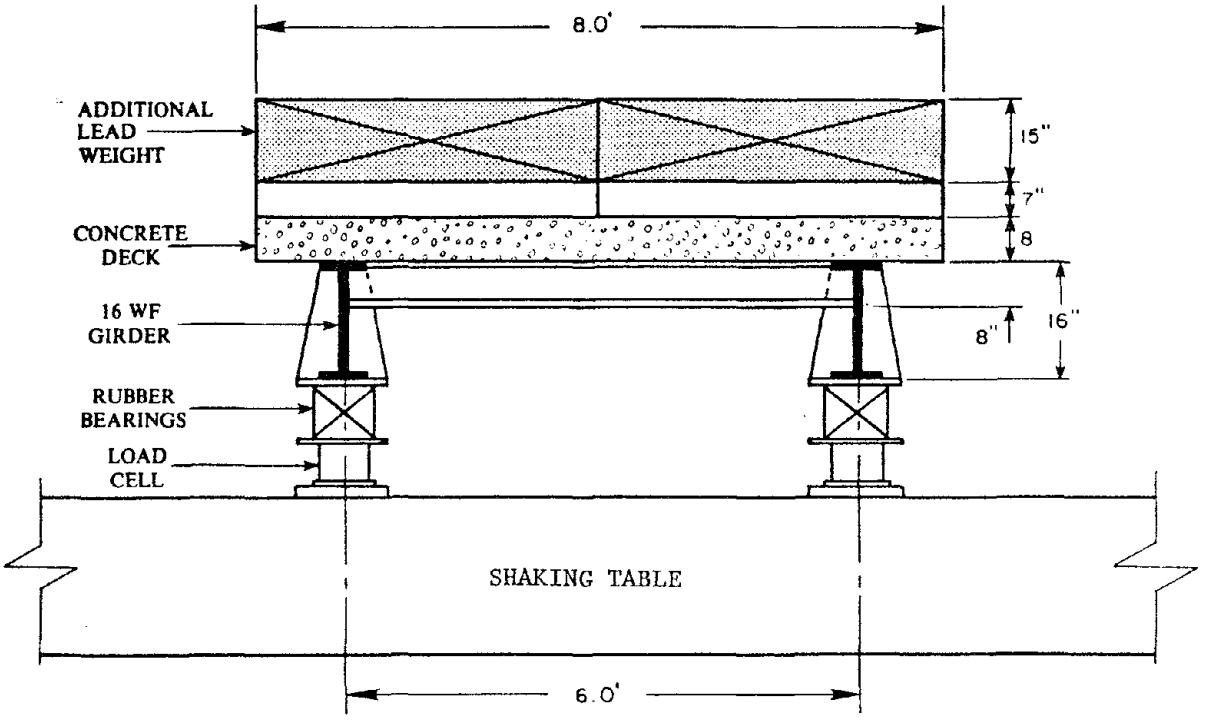

Figure 1 Cross-section of base isolated bridge deck in shaking table tests

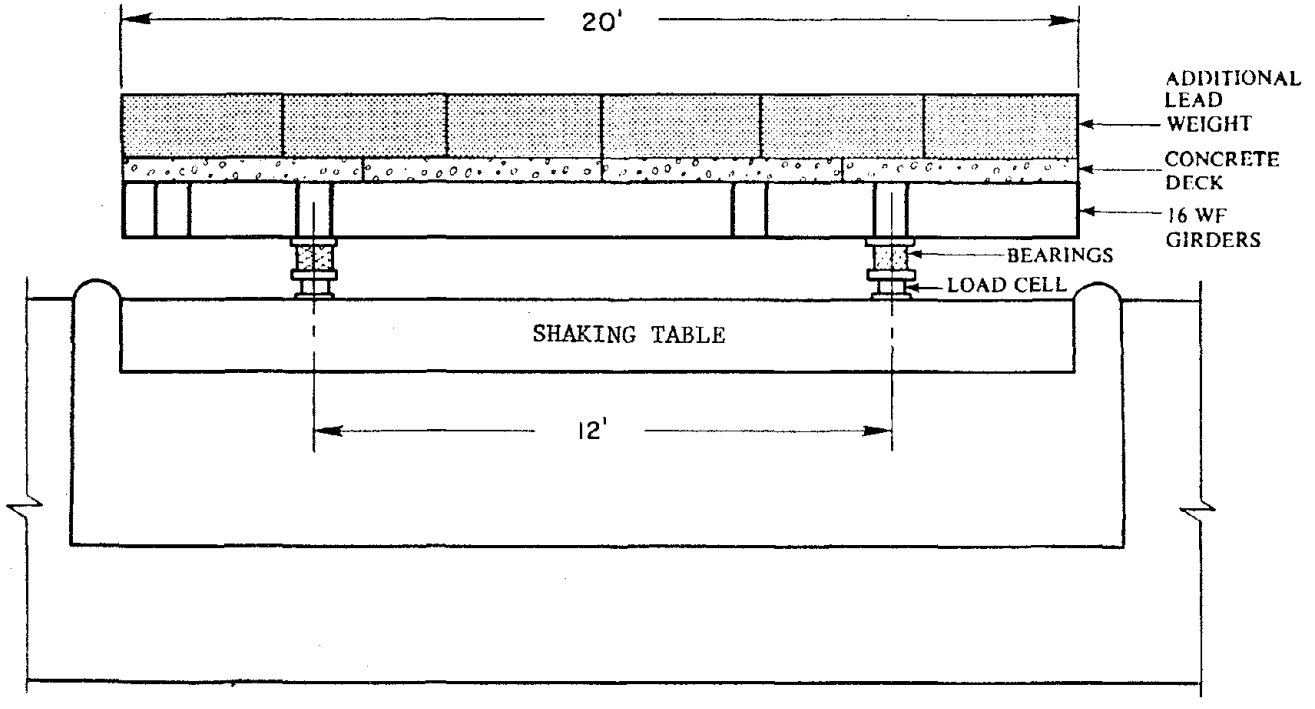

Figure 2 Longitudinal elevation of base isolated bridge deck in shaking table tests

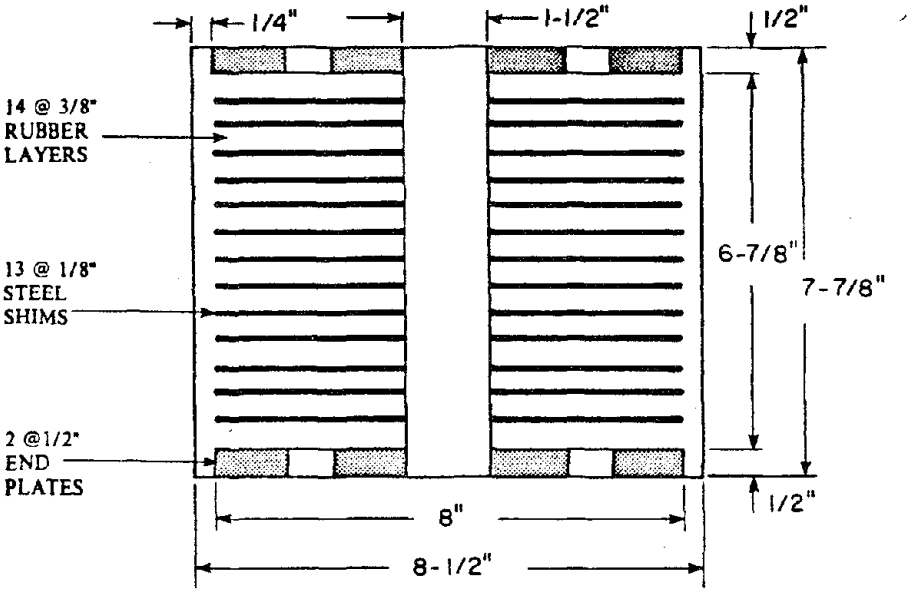

SECTION A-A

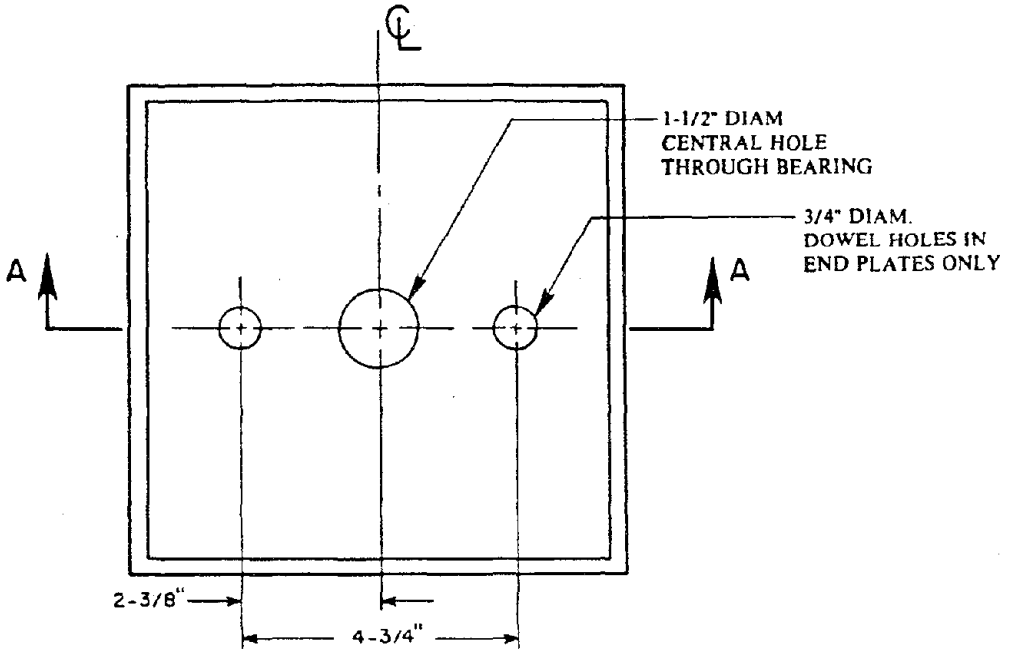

PLAN

Figure 3 Cross-section and plan view of natural rubber isolation bearings

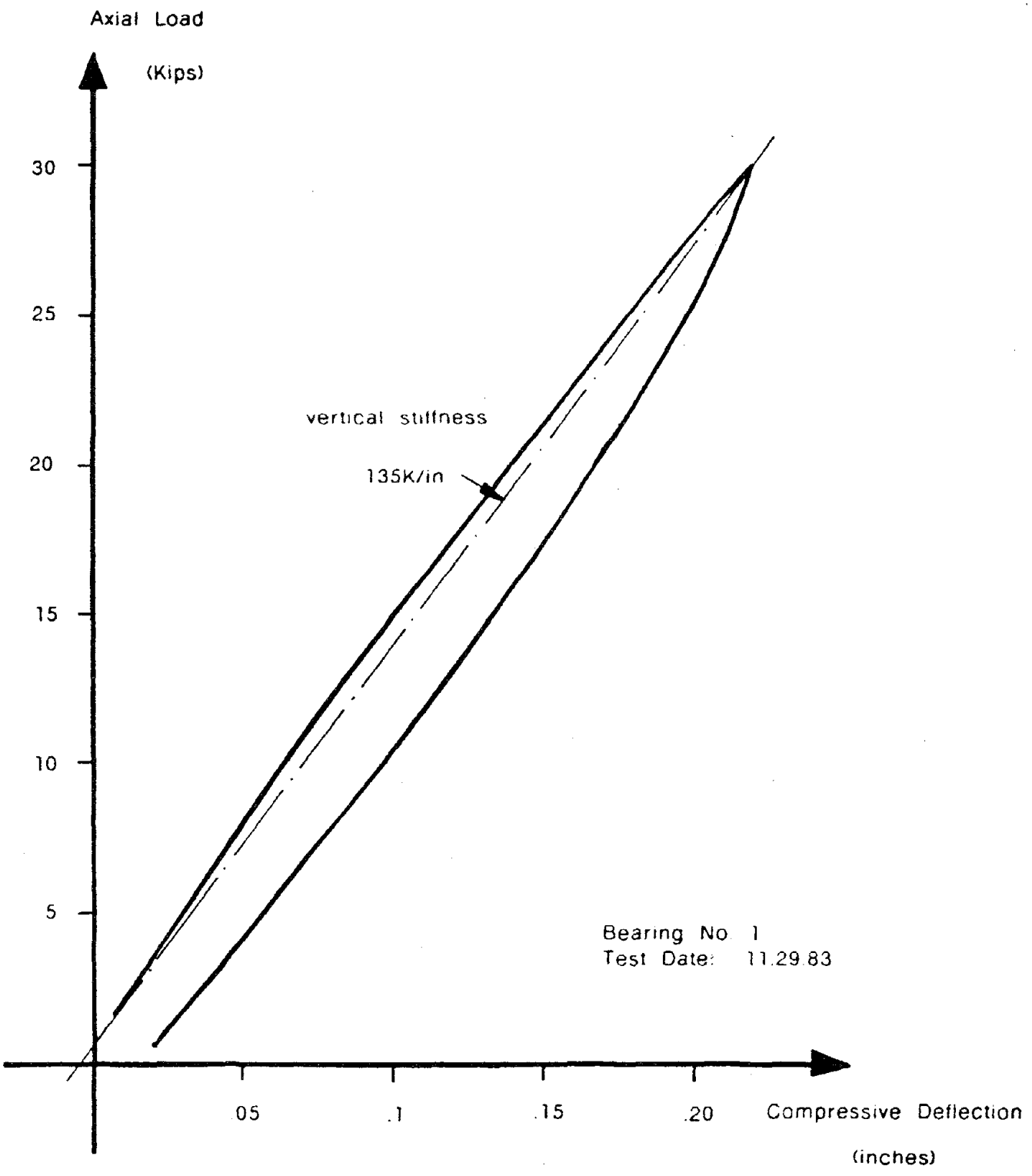

Figure 4 Compressive load-deflection curve for a single rubber bearing

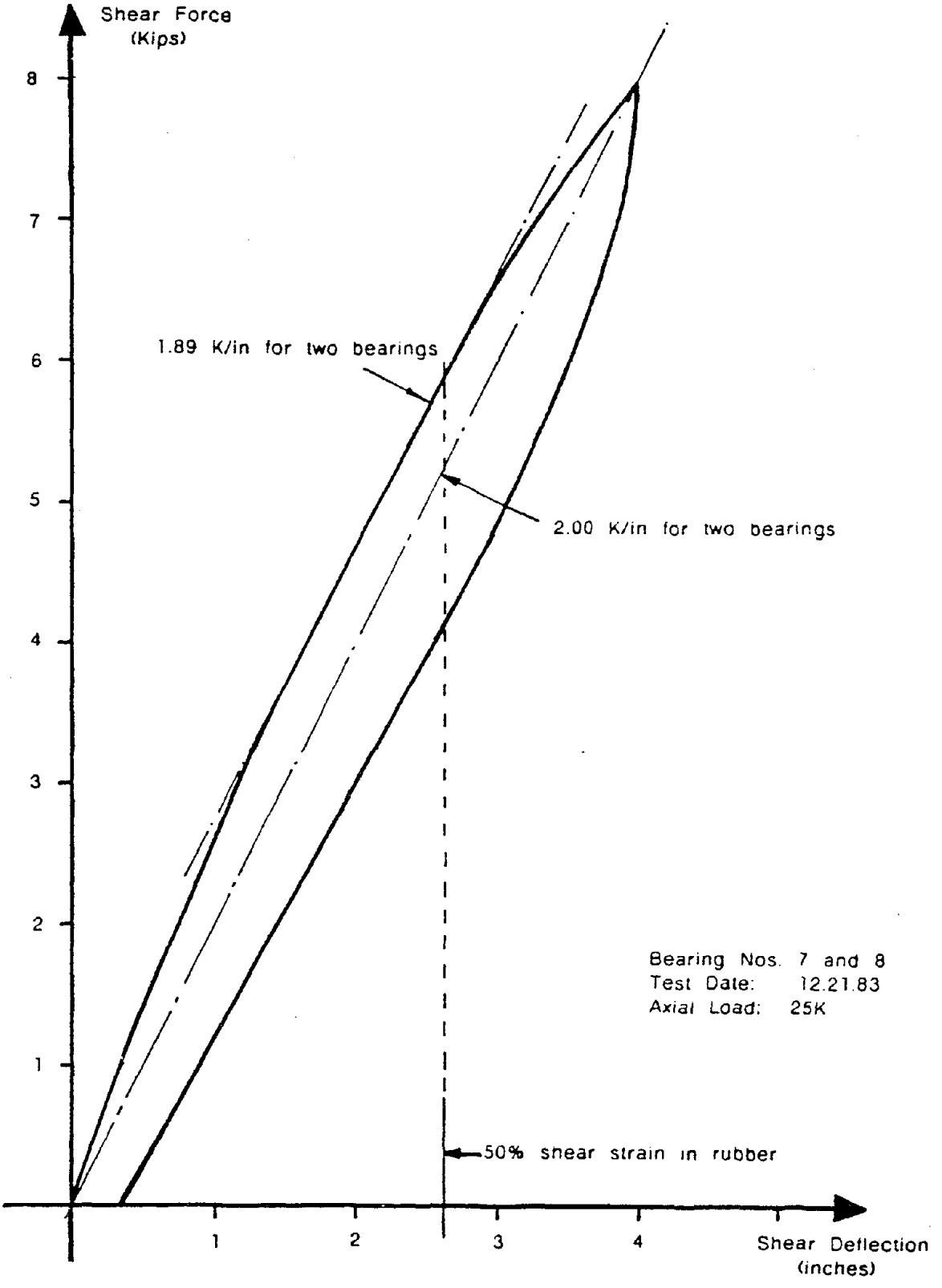

Figure 5 Shear load-deflection curve for two rubber bearings

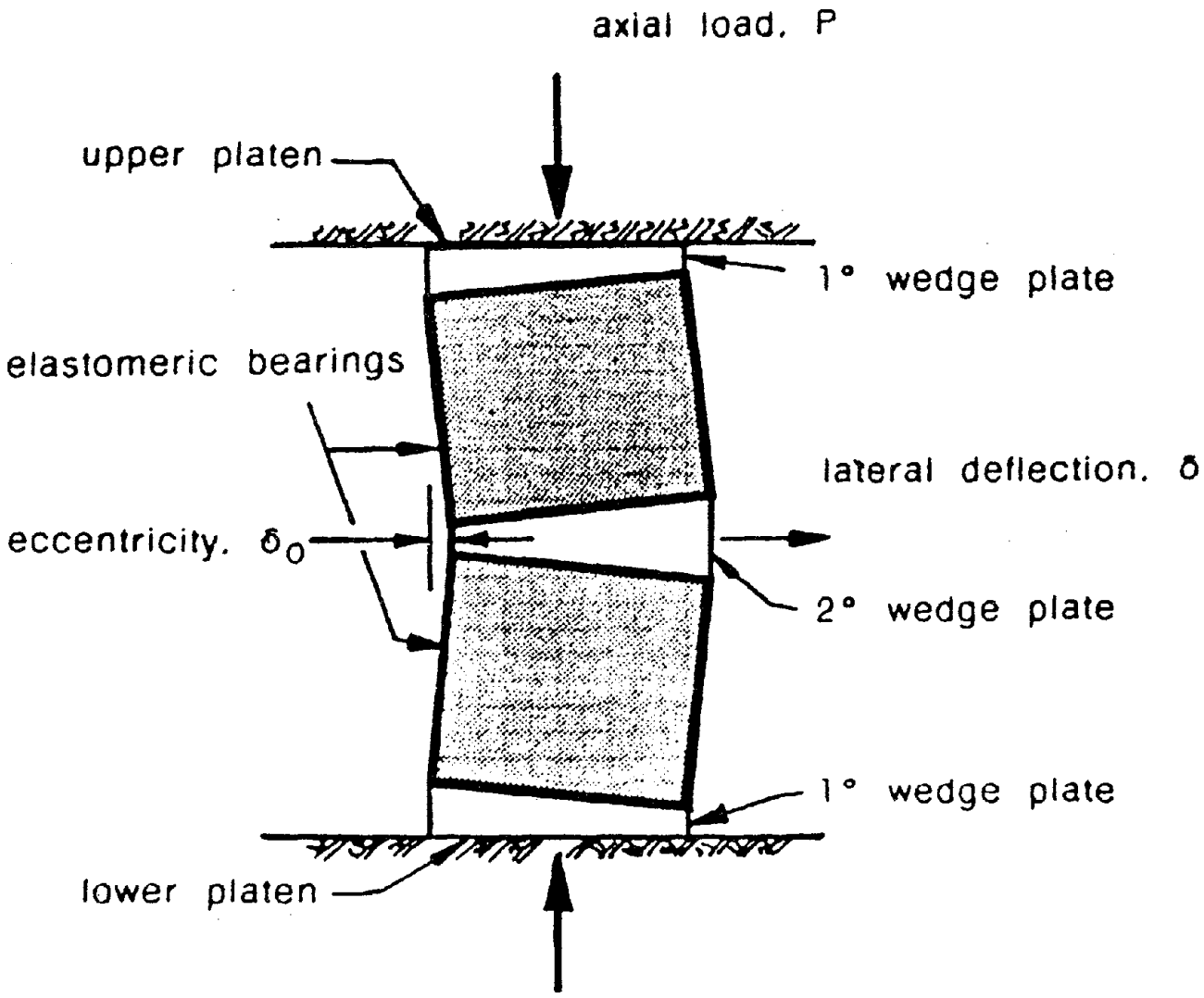

Figure 6 Test arrangement for buckling load determination

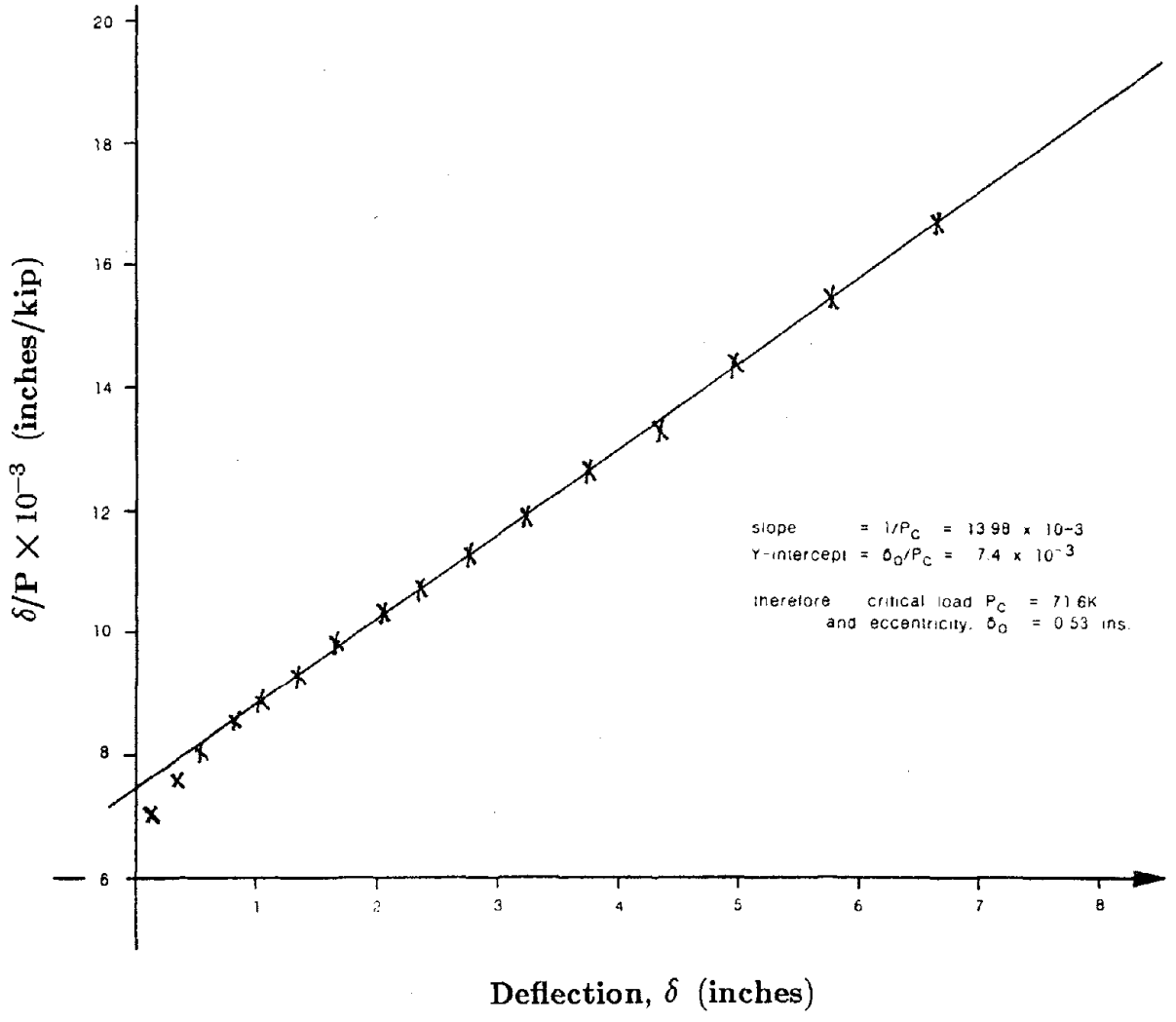

Figure 7 Southwell plot for critical buckling load and initial eccentricity

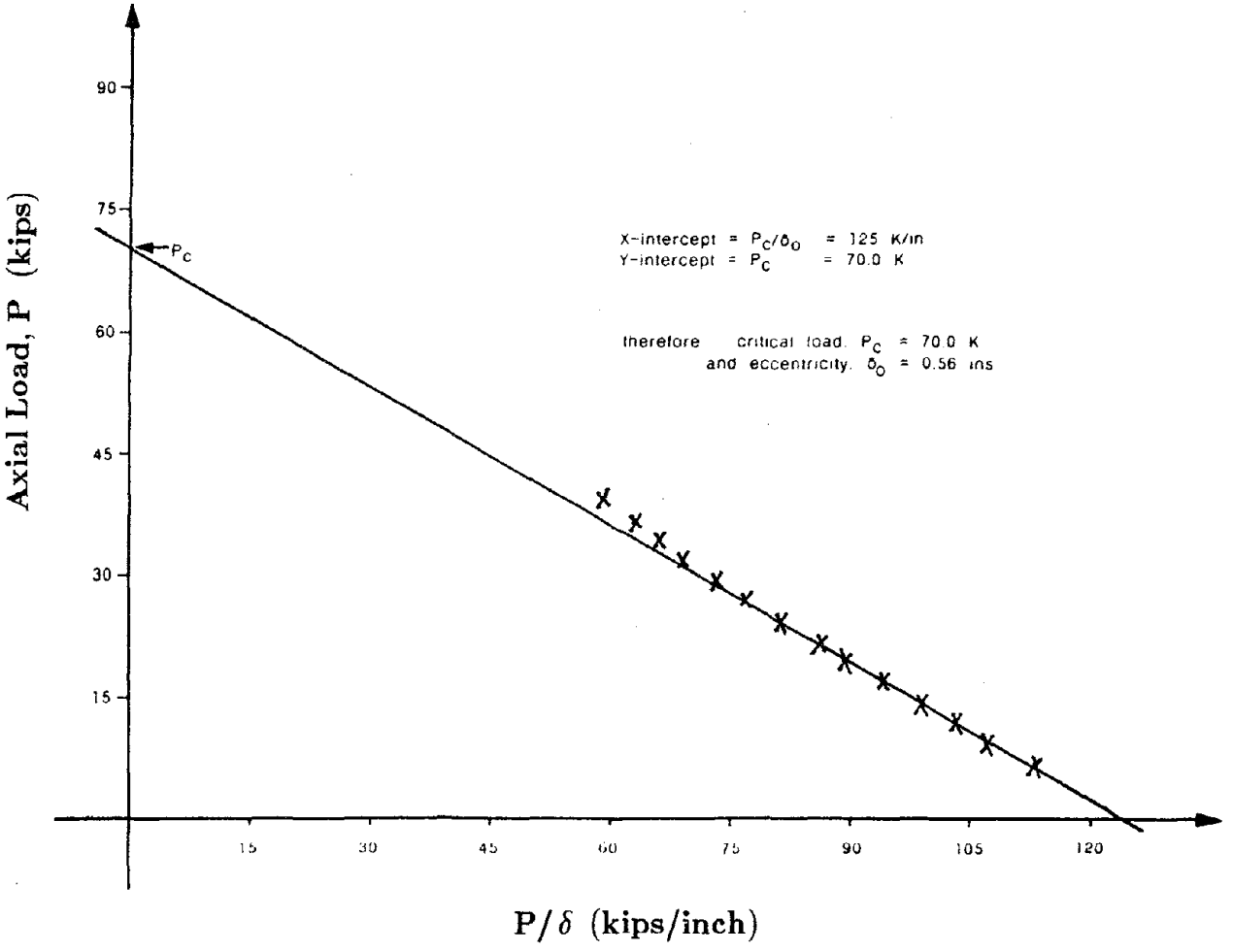

Figure 8 Reversed Southwell plot for critical buckling load and initial eccentricity

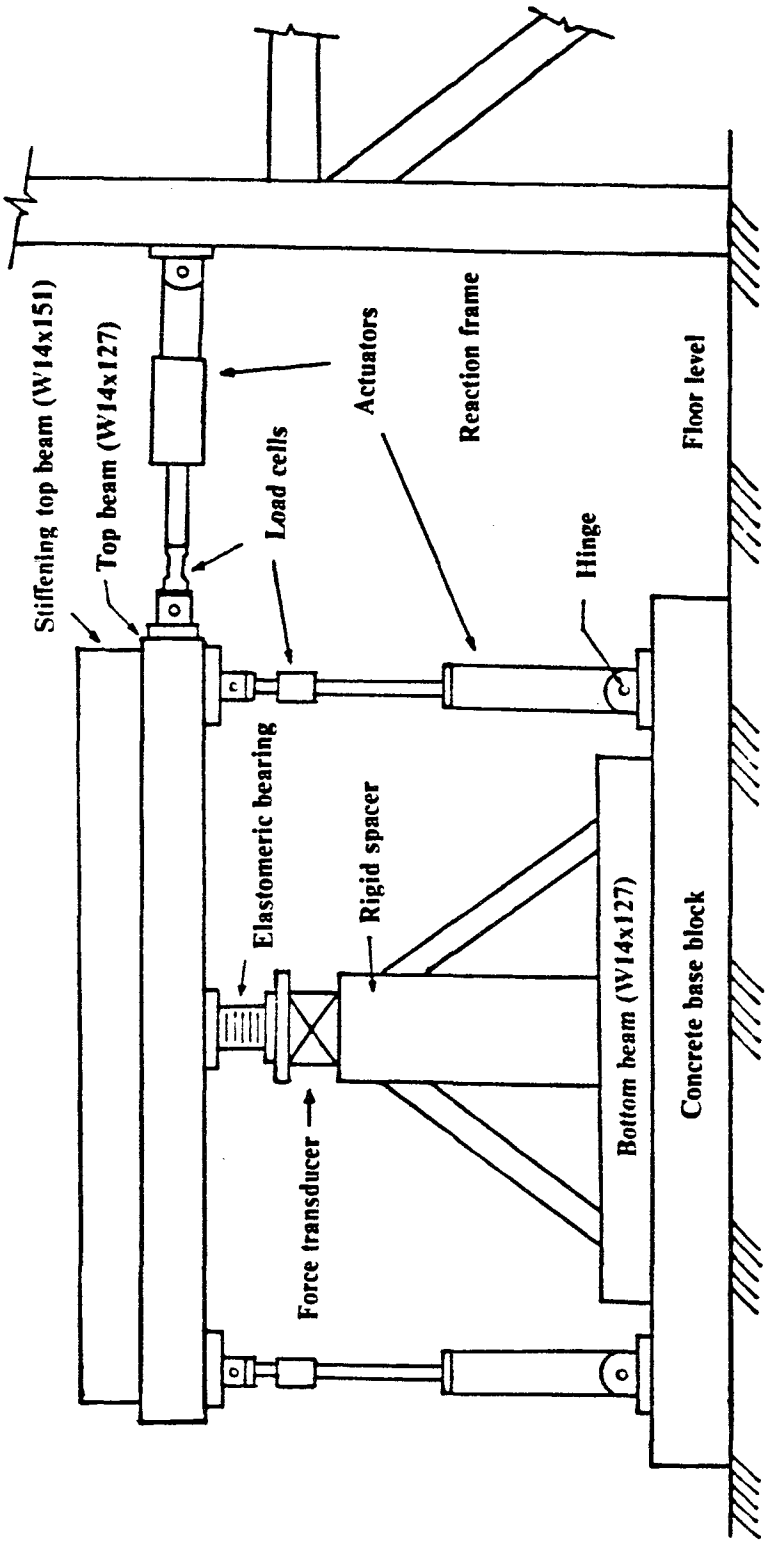

Figure 9 Schematic illustration of setup for cyclic loading tests of a single rubber bearing subjected to compression load

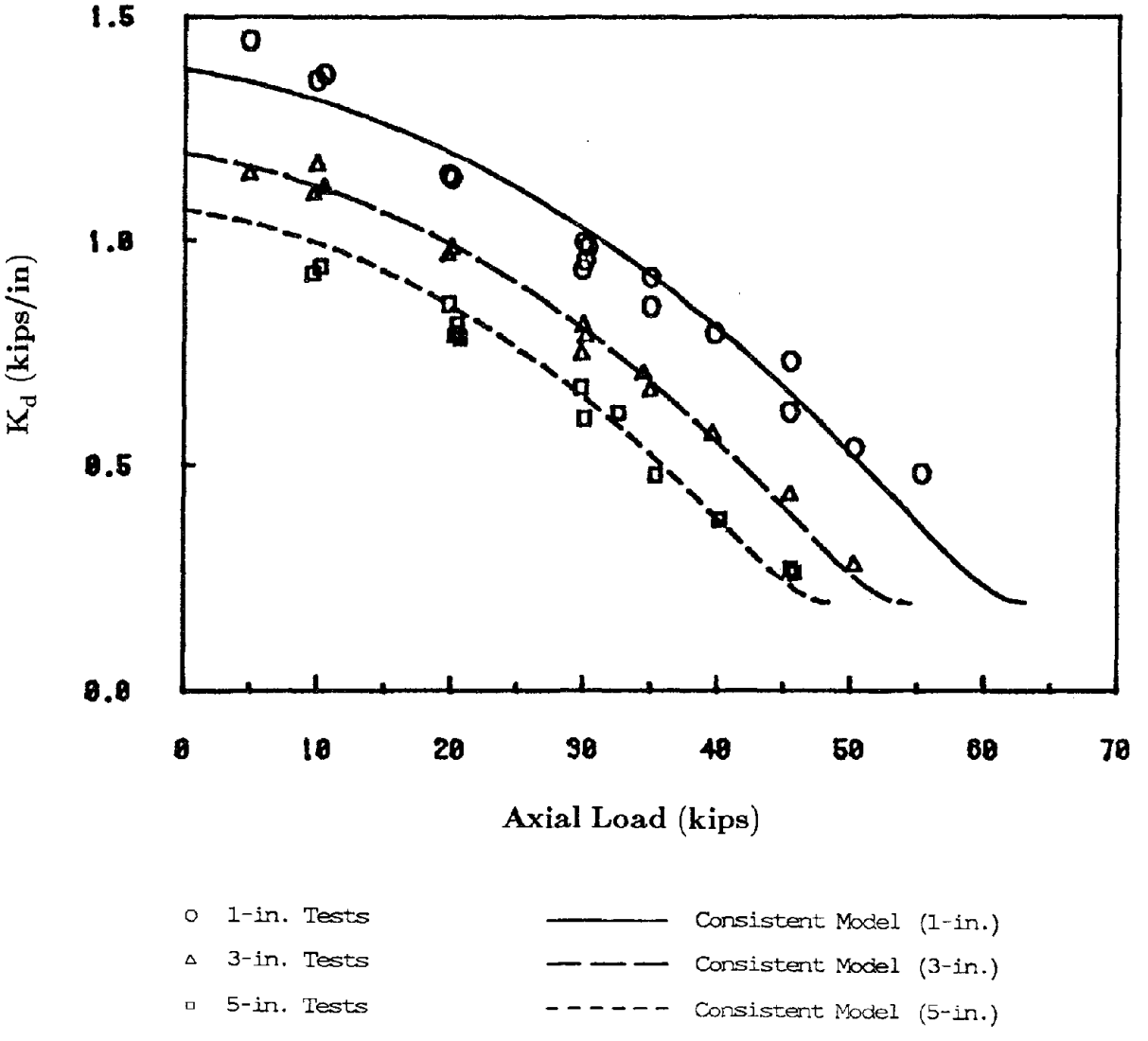

Figure 10 Dynamic shear stiffness of rubber bearing with no lead plug

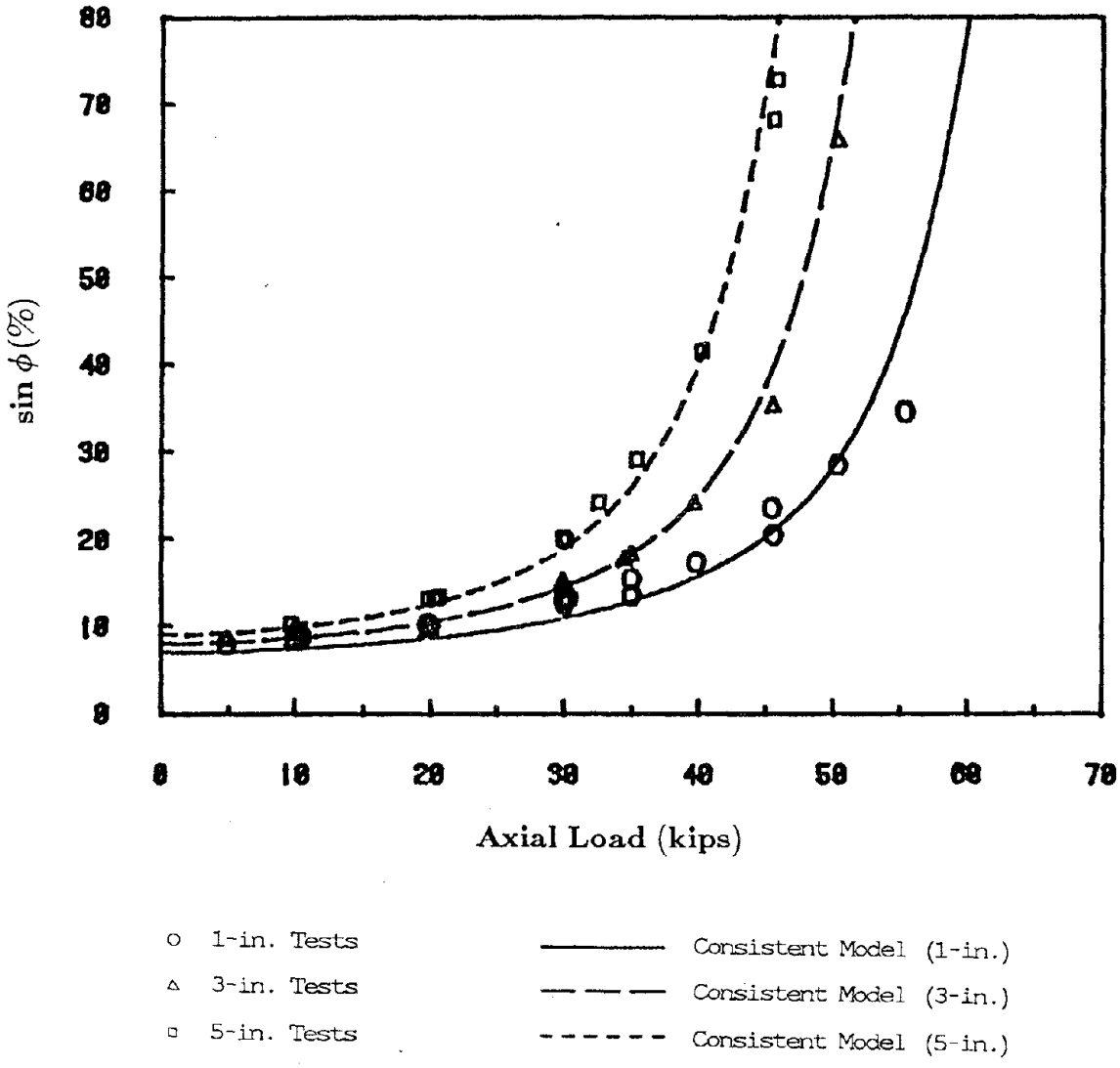

Figure 11 Damping factor of rubber bearing with no lead plug

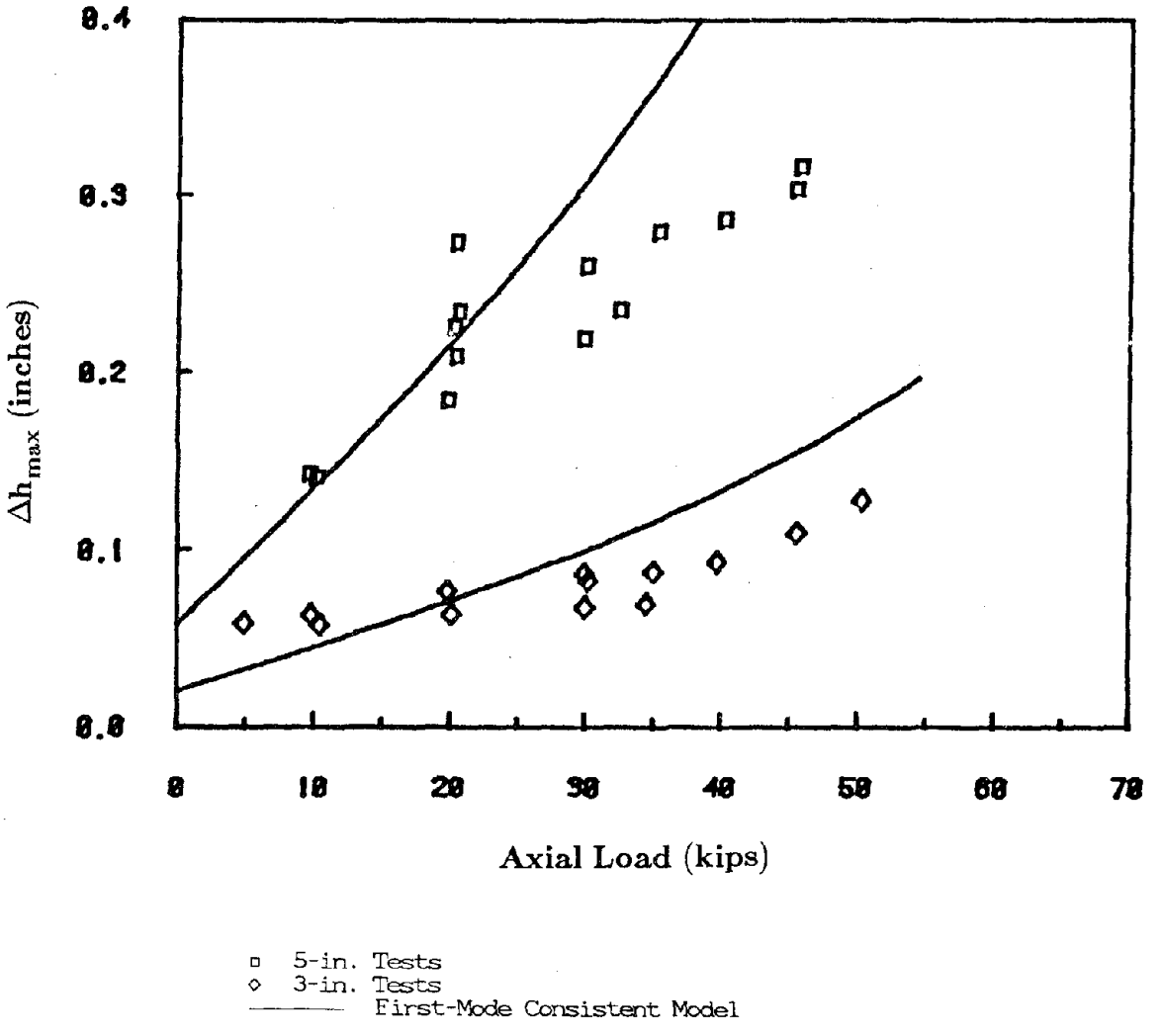

Figure 12 Height reduction of rubber bearing with no lead plug

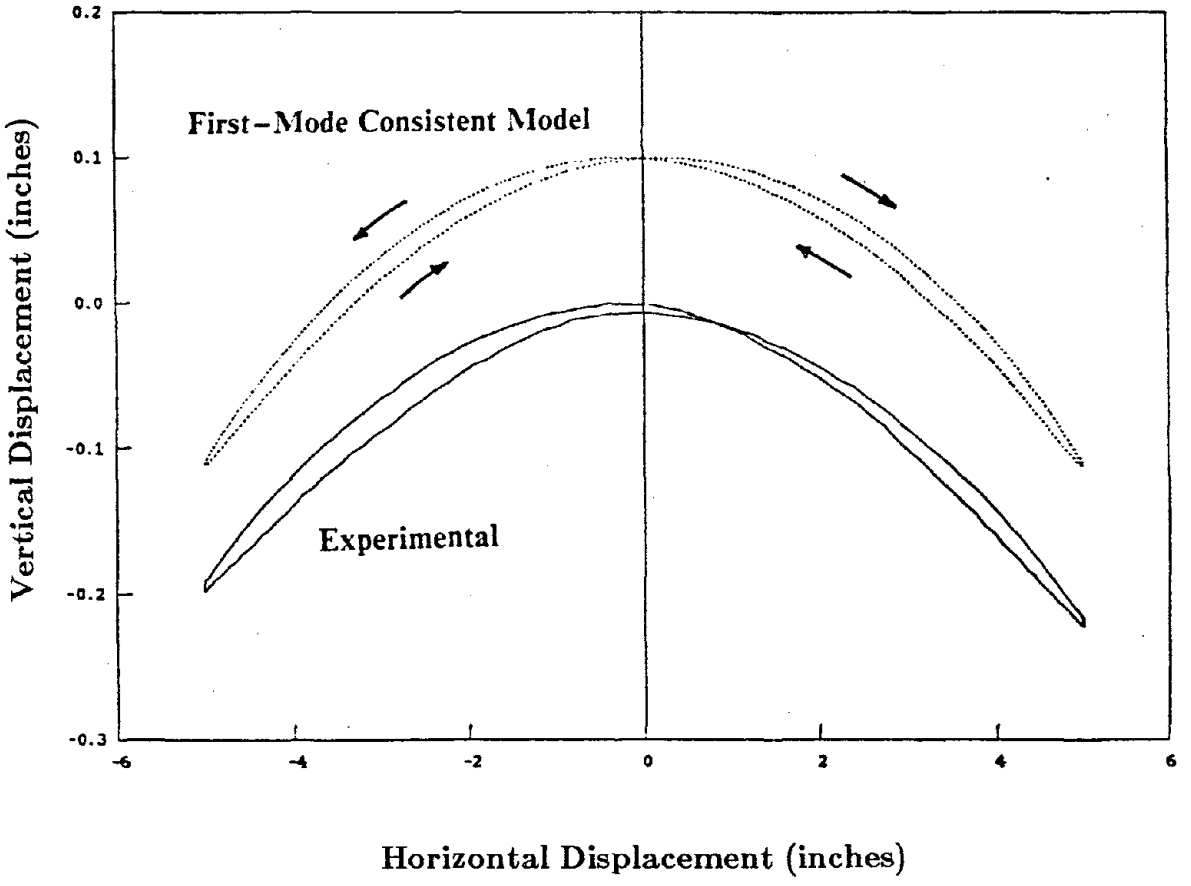

Figure 13 Height reduction loop of rubber bearing at 5 inch displacement cycle
(Note: 0.1 inch is added to the theoretical curve for clarity)

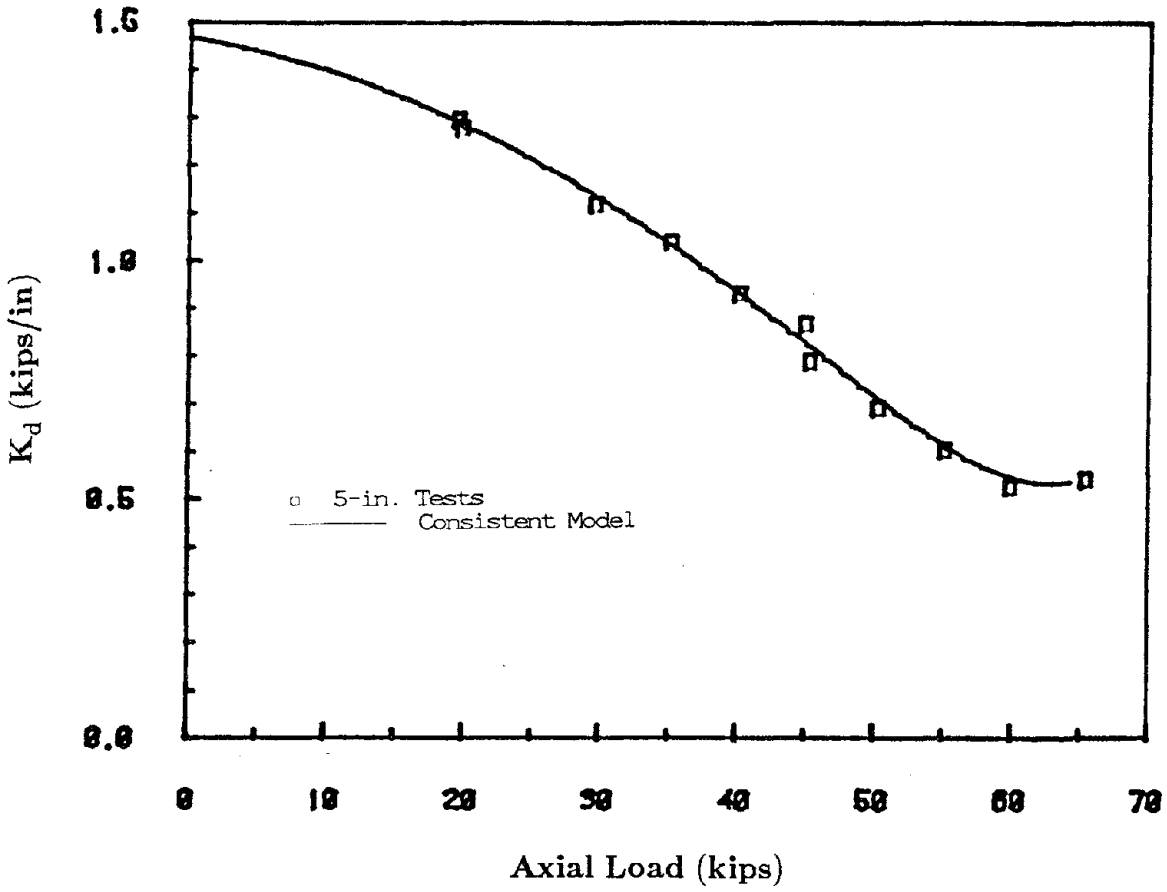

Figure 14 Dynamic shear stiffness of rubber bearing with lead plug

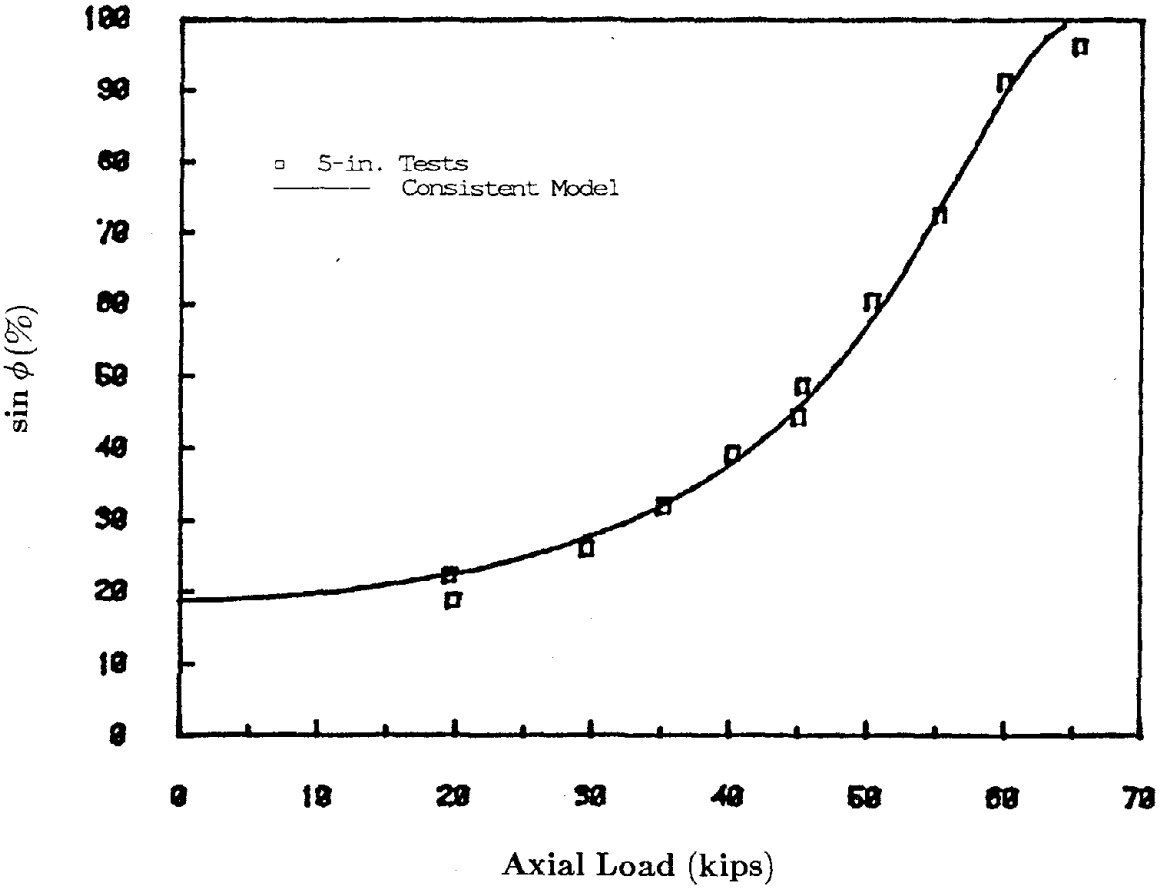

Figure 15 Damping factor of bearing with lead plug

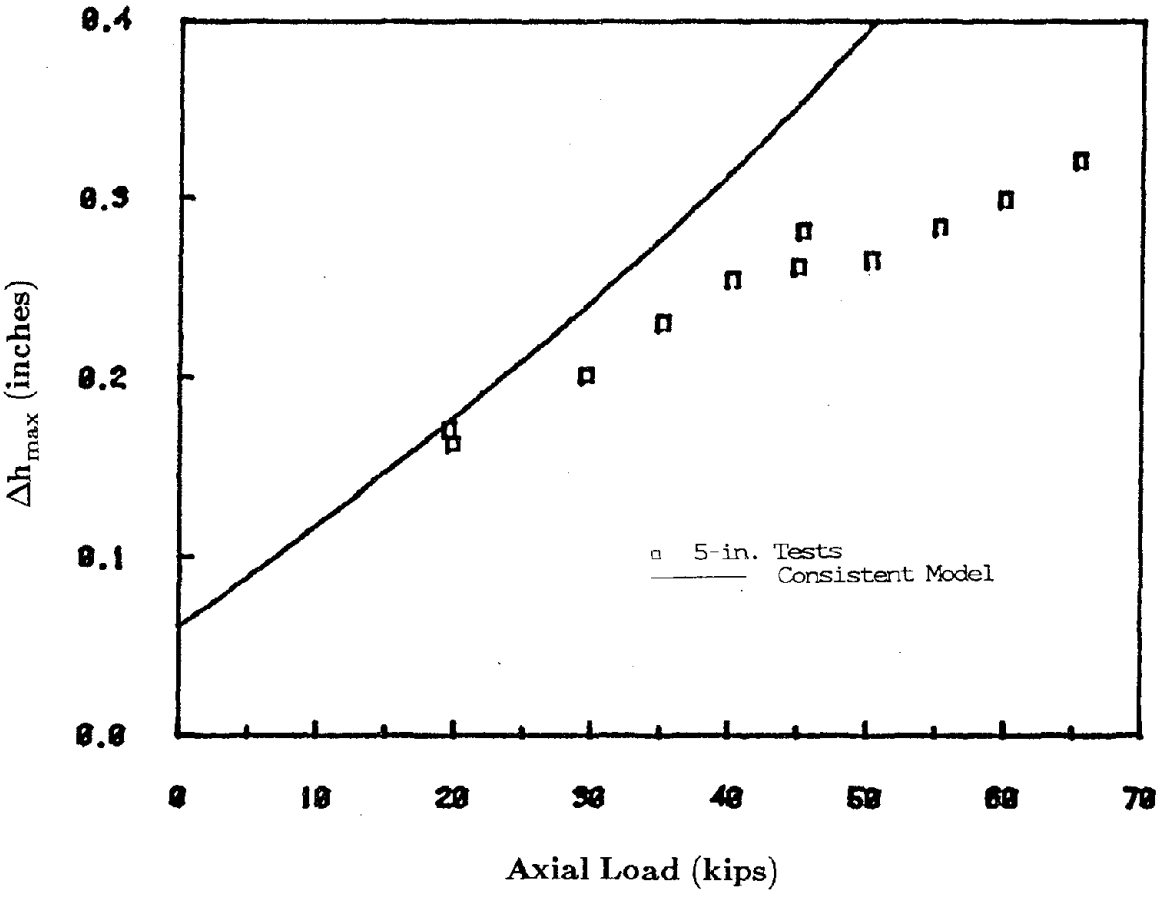

Figure 16 Height reduction of rubber bearing with lead plug

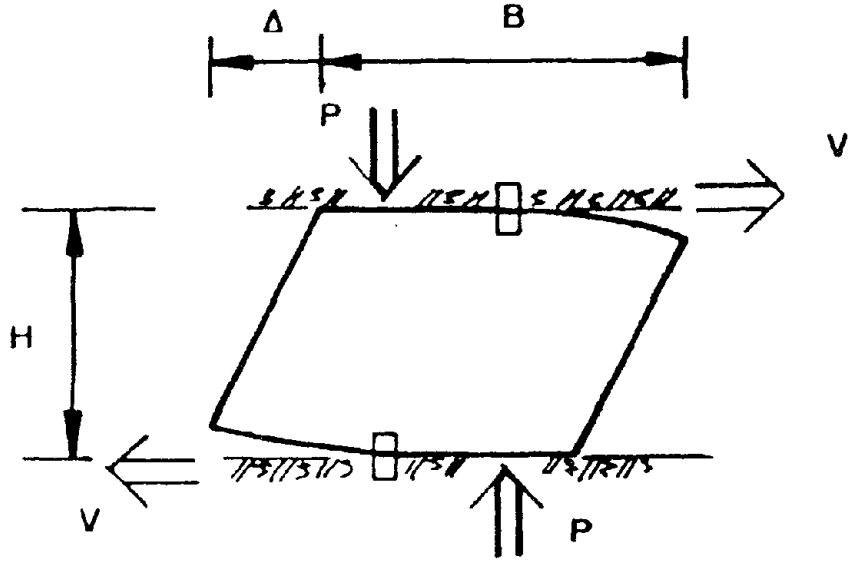

Figure 17 Overturning action in a rubber bearing

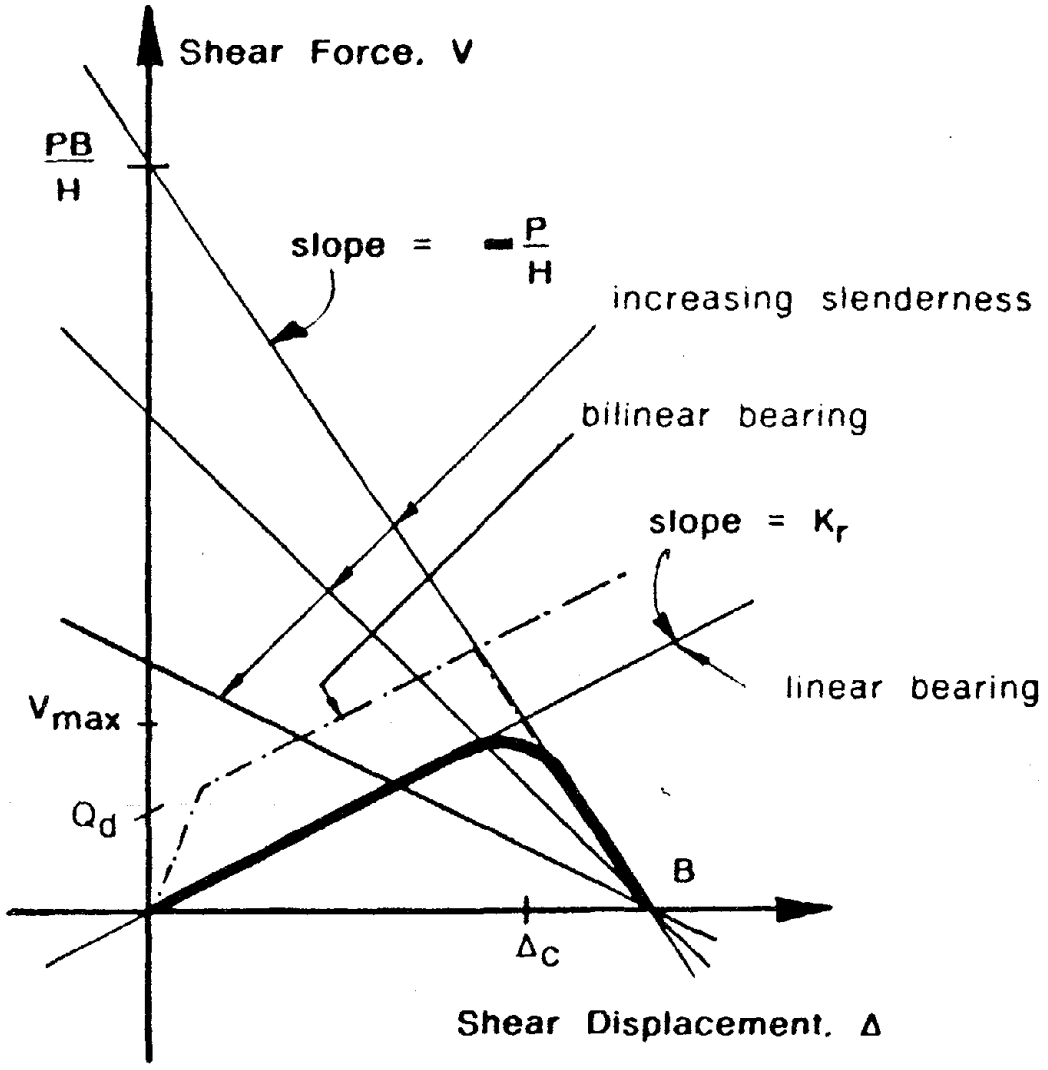

Figure 18 Shear force-displacement diagram showing the limiting effects of overturning

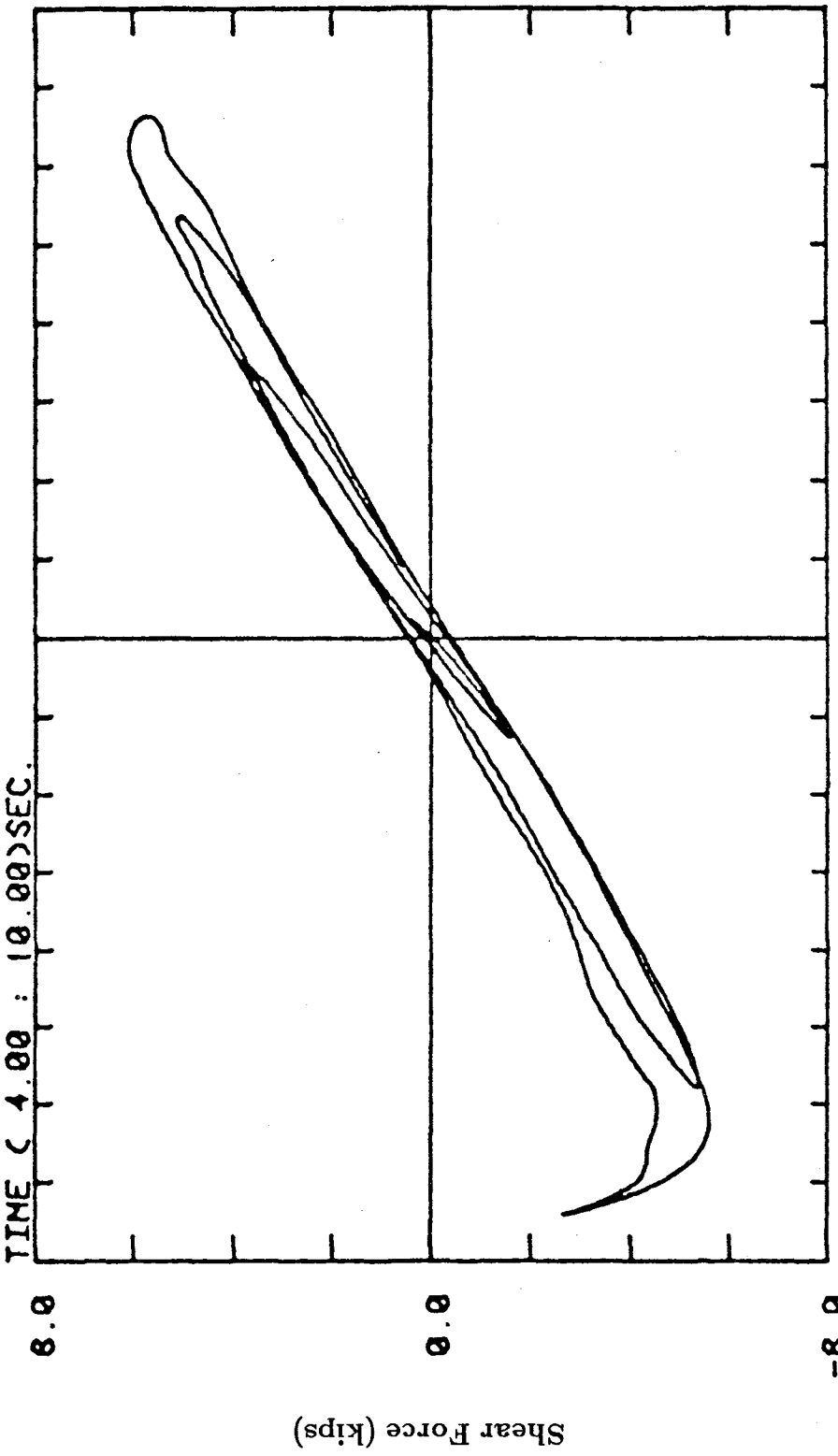

Figure 19 Force-deflection hysteresis loop for a rubber bearing during critical cycles of the ATC-3 (0.32g) synthetic earthquake

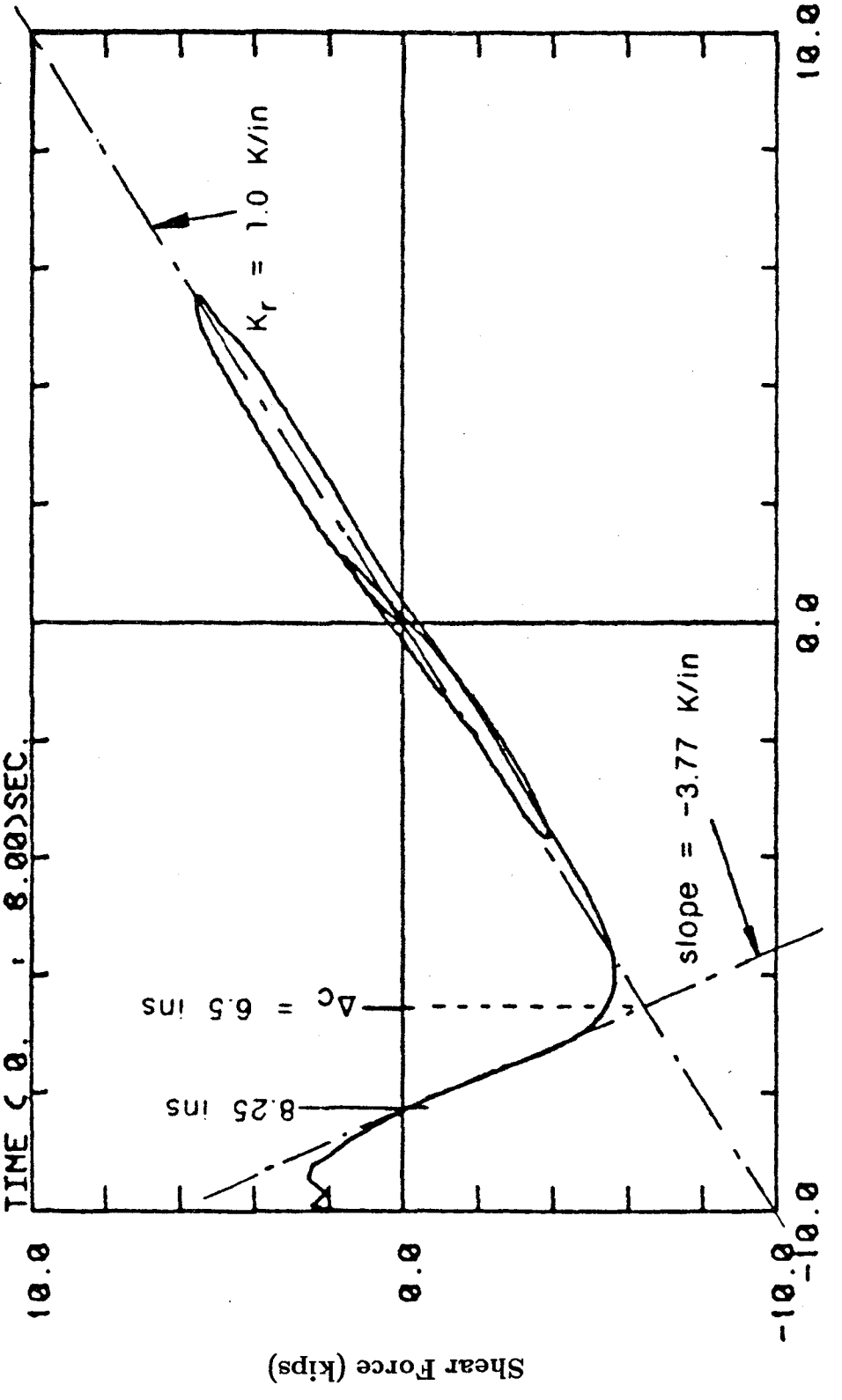

Figure 20 Force-deflection hysteresis loop for a rubber bearing during critical cycles of the El Centro (scaled to 0.94g) earthquake

EARTHQUAKE ENGINEERING RESEARCH CENTER REPORT SERIES

EERC reports are available from the National Information Service for Earthquake Engineering(NISEE) and from the National Technical Information Service(NTIS). Numbers in parentheses are Accession Numbers assigned by the National Technical Information Service; these are followed by a price code. Contact NTIS, 5285 Port Royal Road, Springfield Virginia, 22161 for more information. Reports without Accession Numbers were not available from NTIS at the time of printing. For a current complete list of EERC reports (from EERC 67-1) and availablity information, please contact University of California, EERC, NISEE, 1301 South 46th Street, Richmond, California 94804.

UCB/EERC-80/01 "Earthquake Response of Concrete Gravity Dams Including Hydrodynamic and Foundation Interaction Effects," by Chopra, A.K., Chakrabarti, P. and Gupta, S., January 1980, (AD-A087297)A10.

UCB/EERC-80/02 "Rocking Response of Rigid Blocks to Earthquakes," by Yim, C.S., Chopra, A.K. and Penzien, J., January 1980, (PB80 166 002)A04.

UCB/EERC-80/03 "Optimum Inelastic Design of Seismic-Resistant Reinforced Concrete Frame Structures," by Zagajeski, S.W. and Bertero, V.V., January 1980, (PB80 164 635)A06.

UCB/EERC-80/04 "Effects of Amount and Arrangement of Wall-Panel Reinforcement on Hysteretic Behavior of Reinforced Concrete Walls," by Iliya, R. and Bertero, V.V., February 1980, (PB81 122 525)A09.

UCB/EERC-80/05 "Shaking Table Research on Concrete Dam Models," by Niwa, A. and Clough, R.W., September 1980, (PB81 122 368)A06.

UCB/EERC-80/06 "The Design of Steel Energy-Absorbing Restrainers and their Incorporation into Nuclear Power Plants for Enhanced Safety (Vol 1a): Piping with Energy Absorbing Restrainers: Parameter Study on Small Systems," by Powell, G.H., Oughourlian, C. and Simons, J., June 1980.

UCB/EERC-80/07 "Inelastic Torsional Response of Structures Subjected to Earthquake Ground Motions," by Yamazaki, Y., April 1980, (PB81 122 327)A08.

UCB/EERC-80/08 "Study of X-Braced Steel Frame Structures under Earthquake Simulation," by Ghanaat, Y., April 1980, (PB81 122 335)A11.

UCB/EERC-80/09 "Hybrid Modelling of Soil-Structure Interaction," by Gupta, S., Lin, T.W. and Penzien, J., May 1980, (PB81 122 319)A07.

UCB/EERC-80/10 "General Applicability of a Nonlinear Model of a One Story Steel Frame," by Sveinsson, B.I. and McNiven, H.D., May 1980, (PB81 ,24 877)A06.

UCB/EERC-80/11 "A Green-Function Method for Wave Interaction with a Submerged Body," by Kioka, W., April 1980, (PB81 122 269)A07.

UCB/EERC-80/12 "Hydrodynamic Pressure and Added Mass for Axisymmetric Bodies.," by Nilrat, F., May 1980, (PB81 122 343)A08.

UCB/EERC-80/13 "Treatment of Non-Linear Drag Forces Acting on Offshore Platforms," by Dao, B.V. and Penzien, J., May 1980, (PB81 153 413)A07.

UCB/EERC-80/14 "2D Plane/Axisymmetric Solid Element (Type 3-Elastic or Elastic-Perfectly Plastic)for the ANSR-II Program," by Mondkar, D.P. and Powell, G.H., July 1980, (PB81 122 350)A03.

UCB/EERC-80/15 "A Response Spectrum Method for Random Vibrations," by Der Kiureghian, A., June 1981, (PB81 122 301)A03.

UCB/EERC-80/16 "Cyclic Inelastic Buckling of Tubular Steel Braces," by Zayas, V.A., Popov, E.P. and Mahin, S.A., June 1981, (PB81 124 885)A10.

UCB/EERC-80/17 "Dynamic Response of Simple Arch Dams Including Hydrodynamic Interaction," by Porter, C.S. and Chopra, A.K., July 1981, (PB81 124 000)A13.

UCB/EERC-80/18 "Experimental Testing of a Friction Damped Aseismic Base Isolation System with Fail-Safe Characteristics," by Kelly, J.M., Beucke, K.E. and Skinner, M.S., July 1980, (PB81 148 595)A04.

UCB/EERC-80/19 "The Design of Steel Energy-Absorbing Restrainers and their Incorporation into Nuclear Power Plants for Enhanced Safety (Vol.1B): Stochastic Seismic Analyses of Nuclear Power Plant Structures and Piping Systems Subjected to Multiple Supported Excitations," by Lee, M.C. and Penzien, J., June 1980, (PB82 201 872)A08.

UCB/EERC-80/20 "The Design of Steel Energy-Absorbing Restrainers and their Incorporation into Nuclear Power Plants for Enhanced Safety (Vol 1C): Numerical Method for Dynamic Substructure Analysis," by Dickens, J.M. and Wilson, E.L., June 1980.

UCB/EERC-80/21 "The Design of Steel Energy-Absorbing Restrainers and their Incorporation into Nuclear Power Plants for Enhanced Safety (Vol 2): Development and Testing of Restraints for Nuclear Piping Systems," by Kelly, J.M. and Skinner, M.S., June 1980.

UCB/EERC-80/22 "3D Solid Element (Type 4-Elastic or Elastic-Perfectly-Plastic) for the ANSR-II Program," by Mondkar, D.P. and Powell, G.H., July 1980, (PB81 123 242)A03.

UCB/EERC-80/23 "Gap-Friction Element (Type 5) for the Ansr-II Program," by Mondkar, D.P. and Powell, G.H., July 1980, (PB81 122 285)A03.

UCB/EERC-80/24 "U-Bar Restraint Element (Type 11) for the ANSR-II Program," by Oughourlian, C. and Powell, G.H., July 1980, (PB81 122 293)A03.

UCB/EERC-80/25 "Testing of a Natural Rubber Base Isolation System by an Explosively Simulated Earthquake," by Kelly, J.M., August 1980, (PB81 201 360)A04.

UCB/EERC-80/26 "Input Identification from Structural Vibrational Response," by Hu, Y., August 1980, (PB81 152 308)A05.

UCB/EERC-80/27 "Cyclic Inelastic Behavior of Steel Offshore Structures," by Zayas, V.A., Mahin, S.A. and Popov, E.P., August 1980, (PB81 196 180)A15.

UCB/EERC-80/28 "Shaking Table Testing of a Reinforced Concrete Frame with Biaxial Response," by Oliva, M.G., October 1980, (PB81 154 304)A10.

UCB/EERC-80/29 "Dynamic Properties of a Twelve-Story Prefabricated Panel Building," by Bouwkamp, J.G., Kollegger, J.P. and Stephen, R.M., October 1980, (PB82 138 777)A07.

UCB/EERC-80/30 "Dynamic Properties of an Eight-Story Prefabricated Panel Building," by Bouwkamp, J.G., Kollegger, J.P. and Stephen, R.M., October 1980, (PB81 200 313)A05.

UCB/EERC-80/31 "Predictive Dynamic Response of Panel Type Structures under Earthquakes," by Kollegger, J.P. and Bouwkamp, J.G., October 1980, (PB81 152 316)A04.

UCB/EERC-80/32 "The Design of Steel Energy-Absorbing Restrainers and their Incorporation into Nuclear Power Plants for Enhanced Safety (Vol 3): Testing of Commercial Steels in Low-Cycle Torsional Fatique," by Spanner, P., Parker, E.R., Jongewaard, E. and Dory, M., 1980.

UCB/EERC-80/33 "The Design of Steel Energy-Absorbing Restrainers and their Incorporation into Nuclear Power Plants for Enhanced Safety (Vol 4): Shaking Table Tests of Piping Systems with Energy-Absorbing Restrainers," by Stiemer, S.F. and Godden, W.G., September 1980, (PB82 201 880)A05.

UCB/EERC-80/34 "The Design of Steel Energy-Absorbing Restrainers and their Incorporation into Nuclear Power Plants for Enhanced Safety (Vol 5): Summary Report," by Spencer, P., 1980.

UCB/EERC-80/35 "Experimental Testing of an Energy-Absorbing Base Isolation System," by Kelly, J.M., Skinner, M.S. and Beucke, K.E., October 1980, (PB81 154 072)A04.

UCB/EERC-80/36 "Simulating and Analyzing Artificial Non-Stationary Earth Ground Motions," by Nau, R.F., Oliver, R.M. and Pister, K.S., October 1980, (PB81 153 397)A04.

UCB/EERC-80/37 "Earthquake Engineering at Berkeley - 1980," by , September 1980, (PB81 205 674)A09.

UCB/EERC-80/38 "Inelastic Seismic Analysis of Large Panel Buildings," by Schricker, V. and Powell, G.H., September 1980, (PB81 154 338)A13.

UCB/EERC-80/39 "Dynamic Response of Embankment, Concrete-Gavity and Arch Dams Including Hydrodynamic Interation," by Hall, J.F. and Chopra, A.K., October 1980, (PB81 152 324)A11.

UCB/EERC-80/40 "Inelastic Buckling of Steel Struts under Cyclic Load Reversal.," by Black, R.G., Wenger, W.A. and Popov, E.P., October 1980, (PB81 154 312)A08.

UCB/EERC-80/41 "Influence of Site Characteristics on Buildings Damage during the October 3,1974 Lima Earthquake," by Repetto, P., Arango, I. and Seed, H.B., September 1980, (PB81 161 739)A05.

UCB/EERC-80/42 "Evaluation of a Shaking Table Test Program on Response Behavior of a Two Story Reinforced Concrete Frame," by Blondet, J.M., Clough, R.W. and Mahin, S.A., December 1980, (PB82 196 544)A11.

UCB/EERC-80/43 "Modelling of Soil-Structure Interaction by Finite and Infinite Elements," by Medina, F., December 1980, (PB81 229 270)A04.

UCB/EERC-81/01 "Control of Seismic Response of Piping Systems and Other Structures by Base Isolation," by Kelly, J.M., January 1981, (PB81 200 735)A05.

UCB/EERC-81/02 "OPTNSR- An Interactive Software System for Optimal Design of Statically and Dynamically Loaded Structures with Nonlinear Response," by Bhatti, M.A., Ciampi, V. and Pister, K.S., January 1981, (PB81 218 851)A09.

UCB/EERC-81/03 "Analysis of Local Variations in Free Field Seismic Ground Motions," by Chen, J.-C., Lysmer, J. and Seed, H.B., January 1981, (AD-A099508)A13.

UCB/EERC-81/04 "Inelastic Structural Modeling of Braced Offshore Platforms for Seismic Loading," by Zayas, V.A., Shing, P.-S.B., Mahin, S.A. and Popov, E.P., January 1981, (PB82 138 777)A07.

UCB/EERC-81/05 "Dynamic Response of Light Equipment in Structures," by Der Kiureghian, A., Sackman, J.L. and Nour-Omid, B., April 1981, (PB81 218 497)A04.

UCB/EERC-81/06 "Preliminary Experimental Investigation of a Broad Base Liquid Storage Tank," by Bouwkamp, J.G., Kollegger, J.P. and Stephen, R.M., May 1981, (PB82 140 385)A03.

UCB/EERC-81/07 "The Seismic Resistant Design of Reinforced Concrete Coupled Structural Walls," by Aktan, A.E. and Bertero, V.V., June 1981, (PB82 113 358)A11.

UCB/EERC-81/08 "Unassigned," by Unassigned, 1981.

UCB/EERC-81/09 "Experimental Behavior of a Spatial Piping System with Steel Energy Absorbers Subjected to a Simulated Differential Seismic Input," by Stiemer, S.F., Godden, W.G. and Kelly, J.M., July 1981, (PB82 201 898)A04.

UCB/EERC-81/10 "Evaluation of Seismic Design Provisions for Masonry in the United States," by Sveinsson, B.I., Mayes, R.L. and McNiven, H.D., August 1981, (PB82 166 075)A08.

UCB/EERC-81/11 "Two-Dimensional Hybrid Modelling of Soil-Structure Interaction," by Tzong, T.-J., Gupta, S. and Penzien, J., August 1981, (PB82 142 118)A04.

UCB/EERC-81/12 "Studies on Effects of Infills in Seismic Resistant R/C Construction," by Brokken, S. and Bertero, V.V., October 1981, (PB82 166 190)A09.

UCB/EERC-81/13 "Linear Models to Predict the Nonlinear Seismic Behavior of a One-Story Steel Frame," by Valdimarsson, H., Shah, A.H. and McNiven, H.D., September 1981, (PB82 138 793)A07.

UCB/EERC-81/14 "TLUSH: A Computer Program for the Three-Dimensional Dynamic Analysis of Earth Dams," by Kagawa, T., Mejia, L.H., Seed, H.B. and Lysmer, J., September 1981, (PB82 139 940)A06.

UCB/EERC-81/15 "Three Dimensional Dynamic Response Analysis of Earth Dams," by Mejia, L.H. and Seed, H.B., September 1981, (PB82 137 274)A12.

UCB/EERC-81/16 "Experimental Study of Lead and Elastomeric Dampers for Base Isolation Systems," by Kelly, J.M. and Hodder, S.B., October 1981, (PB82 166 182)A05.

UCB/EERC-81/17 "The Influence of Base Isolation on the Seismic Response of Light Secondary Equipment," by Kelly, J.M., April 1981, (PB82 255 266)A04.

UCB/EERC-81/18 "Studies on Evaluation of Shaking Table Response Analysis Procedures," by Blondet, J. M., November 1981, (PB82 197 278)A10.

UCB/EERC-81/19 "DELIGHT.STRUCT: A Computer-Aided Design Environment for Structural Engineering," by Balling, R.J., Pister, K.S. and Polak, E., December 1981, (PB82 218 496)A07.

UCB/EERC-81/20 "Optimal Design of Seismic-Resistant Planar Steel Frames," by Balling, R.J., Ciampi, V. and Pister, K.S., December 1981, (PB82 220 179)A07.

UCB/EERC-82/01 "Dynamic Behavior of Ground for Seismic Analysis of Lifeline Systems," by Sato, T. and Der Kiureghian, A., January 1982, (PB82 218 926)A05.

UCB/EERC-82/02 "Shaking Table Tests of a Tubular Steel Frame Model," by Ghanaat, Y. and Clough, R.W., January 1982, (PB82 220 161)A07.

UCB/EERC-82/03 "Behavior of a Piping System under Seismic Excitation: Experimental Investigations of a Spatial Piping System supported by Mechanical Shock Arrestors," by Schneider, S., Lee, H.-M. and Godden, W. G., May 1982, (PB83 172 544)A09.

UCB/EERC-82/04 "New Approaches for the Dynamic Analysis of Large Structural Systems," by Wilson, E.L., June 1982, (PB83 148 080)A05.

UCB/EERC-82/05 "Model Study of Effects of Damage on the Vibration Properties of Steel Offshore Platforms," by Shahrivar, F. and Bouwkamp, J.G., June 1982, (PB83 148 742)A10.

UCB/EERC-82/06 "States of the Art and Pratice in the Optimum Seismic Design and Analytical Response Prediction of R/C Frame Wall Structures," by Aktan, A.E. and Bertero, V.V., July 1982, (PB83 147 736)A05.

UCB/EERC-82/07 "Further Study of the Earthquake Response of a Broad Cylindrical Liquid-Storage Tank Model," by Manos, G.C. and Clough, R.W., July 1982, (PB83 147 744)A11.

UCB/EERC-82/08 "An Evaluation of the Design and Analytical Seismic Response of a Seven Story Reinforced Concrete Frame," by Charney, F.A. and Bertero, V.V., July 1982, (PB83 157 628)A09.

UCB/EERC-82/09 "Fluid-Structure Interactions: Added Mass Computations for Incompressible Fluid," by Kuo, J.S.-H., August 1982, (PB83 156 281)A07.

UCB/EERC-82/10 "Joint-Opening Nonlinear Mechanism: Interface Smeared Crack Model," by Kuo, J.S.-H., August 1982, (PB83 149 195)A05.

UCB/EERC-82/11 "Dynamic Response Analysis of Techi Dam," by Clough, R.W., Stephen, R.M. and Kuo, J.S.-H., August 1982, (PB83 147 496)A06.

UCB/EERC-82/12 "Prediction of the Seismic Response of R/C Frame-Coupled Wall Structures," by Aktan, A.E., Bertero, V.V. and Piazzo, M., August 1982, (PB83 149 203)A09.

UCB/EERC-82/13 "Preliminary Report on the Smart 1 Strong Motion Array in Taiwan," by Bolt, B.A., Loh, C.H., Penzien, J. and Tsai, Y.B., August 1982, (PB83 159 400)A10.

UCB/EERC-82/14 "Shaking-Table Studies of an Eccentrically X-Braced Steel Structure," by Yang, M.S., September 1982, (PB83 260 778)A12.

UCB/EERC-82/15 "The Performance of Stairways in Earthquakes," by Roha, C., Axley, J.W. and Bertero, V.V., September 1982, (PB83 157 693)A07.

UCB/EERC-82/16 "The Behavior of Submerged Multiple Bodies in Earthquakes," by Liao, W.-G., September 1982, (PB83 158 709)A07.

UCB/EERC-82/17 "Effects of Concrete Types and Loading Conditions on Local Bond-Slip Relationships," by Cowell, A.D., Popov, E.P. and Bertero, V.V., September 1982, (PB83 153 577)A04.

UCB/EERC-82/18 "Mechanical Behavior of Shear Wall Vertical Boundary Members: An Experimental Investigation," by Wagner, M.T. and Bertero, V.V., October 1982, (PB83 159 764)A05.

UCB/EERC-82/19 "Experimental Studies of Multi-support Seismic Loading on Piping Systems," by Kelly, J.M. and Cowell, A.D., November 1982.

UCB/EERC-82/20 "Generalized Plastic Hinge Concepts for 3D Beam-Column Elements," by Chen, P. F.-S. and Powell, G.H., November 1982, (PB83 247 981)A13.

UCB/EERC-82/21 "ANSR-II: General Computer Program for Nonlinear Structural Analysis," by Oughourlian, C.V. and Powell, G.H., November 1982, (PB83 251 330)A12.

UCB/EERC-82/22 "Solution Strategies for Statically Loaded Nonlinear Structures," by Simons, J.W. and Powell, G.H., November 1982, (PB83 197 970)A06.

UCB/EERC-82/23 "Analytical Model of Deformed Bar Anchorages under Generalized Excitations," by Ciampi, V., Eligehausen, R., Bertero, V.V. and Popov, E.P., November 1982, (PB83 169 532)A06.

UCB/EERC-82/24 "A Mathematical Model for the Response of Masonry Walls to Dynamic Excitations," by Sucuoglu, H., Mengi, Y. and McNiven, H.D., November 1982, (PB83 169 011)A07.

UCB/EERC-82/25 "Earthquake Response Considerations of Broad Liquid Storage Tanks," by Cambra, F.J., November 1982, (PB83 251 215)A09.

UCB/EERC-82/26 "Computational Models for Cyclic Plasticity, Rate Dependence and Creep," by Mosaddad, B. and Powell, G.H., November 1982, (PB83 245 829)A08.

UCB/EERC-82/27 "Inelastic Analysis of Piping and Tubular Structures," by Mahasuverachai, M. and Powell, G.H., November 1982, (PB83 249 987)A07.

UCB/EERC-83/01 "The Economic Feasibility of Seismic Rehabilitation of Buildings by Base Isolation," by Kelly, J.M., January 1983, (PB83 197 988)A05.

UCB/EERC-83/02 "Seismic Moment Connections for Moment-Resisting Steel Frames.," by Popov, E.P., January 1983, (PB83 195 412)A04.

UCB/EERC-83/03 "Design of Links and Beam-to-Column Connections for Eccentrically Braced Steel Frames," by Popov, E.P. and Malley, J.O., January 1983, (PB83 194 811)A04.

UCB/EERC-83/04 "Numerical Techniques for the Evaluation of Soil-Structure Interaction Effects in the Time Domain," by Bayo, E. and Wilson, E.L., February 1983, (PB83 245 605)A09.

UCB/EERC-83/05 "A Transducer for Measuring the Internal Forces in the Columns of a Frame-Wall Reinforced Concrete Structure," by Sause, R. and Bertero, V.V., May 1983, (PB84 119 494)A06.

UCB/EERC-83/06 "Dynamic Interactions Between Floating Ice and Offshore Structures," by Croteau, P., May 1983, (PB84 119 486)A16.

UCB/EERC-83/07 "Dynamic Analysis of Multiply Tuned and Arbitrarily Supported Secondary Systems," by Igusa, T. and Der Kiureghian, A., July 1983, (PB84 118 272)A11.

UCB/EERC-83/08 "A Laboratory Study of Submerged Multi-body Systems in Earthquakes," by Ansari, G.R., June 1983, (PB83 261 842)A17.

UCB/EERC-83/09 "Effects of Transient Foundation Uplift on Earthquake Response of Structures," by Yim, C.-S. and Chopra, A.K., June 1983, (PB83 261 396)A07.

UCB/EERC-83/10 "Optimal Design of Friction-Braced Frames under Seismic Loading," by Austin, M.A. and Pister, K.S., June 1983, (PB84 119 288)A06.

UCB/EERC-83/11 "Shaking Table Study of Single-Story Masonry Houses: Dynamic Performance under Three Component Seismic Input and Recommendations," by Manos, G.C., Clough, R.W. and Mayes, R.L., July 1983, (UCB/EERC-83/11)A08.

UCB/EERC-83/12 "Experimental Error Propagation in Pseudodynamic Testing," by Shiing, P.B. and Mahin, S.A., June 1983, (PB84 119 270)A09.

UCB/EERC-83/13 "Experimental and Analytical Predictions of the Mechanical Characteristics of a 1/5-scale Model of a 7-story R/C Frame-Wall Building Structure," by Aktan, A.E., Bertero, V.V., Chowdhury, A.A. and Nagashima, T., June 1983, (PB84 119 213)A07.

UCB/EERC-83/14 "Shaking Table Tests of Large-Panel Precast Concrete Building System Assemblages," by Oliva, M.G. and Clough, R.W., June 1983, (PB86 110 210/AS)A11.

UCB/EERC-83/15 "Seismic Behavior of Active Beam Links in Eccentrically Braced Frames," by Hjelmstad, K.D. and Popov, E.P., July 1983, (PB84 119 676)A09.

UCB/EERC-83/16 "System Identification of Structures with Joint Rotation," by Dimsdale, J.S., July 1983, (PB84 192 210)A06.

UCB/EERC-83/17 "Construction of Inelastic Response Spectra for Single-Degree-of-Freedom Systems," by Mahin, S. and Lin, J., June 1983, (PB84 208 834)A05.

UCB/EERC-83/18 "Interactive Computer Analysis Methods for Predicting the Inelastic Cyclic Behaviour of Structural Sections," by Kaba, S. and Mahin, S., July 1983, (PB84 192 012)A06.

UCB/EERC-83/19 "Effects of Bond Deterioration on Hysteretic Behavior of Reinforced Concrete Joints," by Filippou, F.C., Popov, E.P. and Bertero, V.V., August 1983, (PB84 192 020)A10.

UCB/EERC-83/20 "Correlation of Analytical and Experimental Responses of Large-Panel Precast Building Systems," by Oliva, M.G., Clough, R.W., Velkov, M. and Gavrilovic, P., May 1988.

UCB/EERC-83/21 "Mechanical Characteristics of Materials Used in a 1/5 Scale Model of a 7-Story Reinforced Concrete Test Structure," by Bertero, V.V., Aktan, A.E., Harris, H.G. and Chowdhury, A.A., October 1983, (PB84 193 697)A05.

UCB/EERC-83/22 "Hybrid Modelling of Soil-Structure Interaction in Layered Media," by Tzong, T.-J. and Penzien, J., October 1983, (PB84 192 178)A08.

UCB/EERC-83/23 "Local Bond Stress-Slip Relationships of Deformed Bars under Generalized Excitations," by Eligehausen, R., Popov, E.P. and Bertero, V.V., October 1983, (PB84 192 848)A09.

UCB/EERC-83/24 "Design Considerations for Shear Links in Eccentrically Braced Frames," by Malley, J.O. and Popov, E.P., November 1983, (PB84 192 186)A07.

UCB/EERC-84/01 "Pseudodynamic Test Method for Seismic Performance Evaluation: Theory and Implementation," by Shing, P.-S.B. and Mahin, S.A., January 1984, (PB84 190 644)A08.

UCB/EERC-84/02 "Dynamic Response Behavior of Kiang Hong Dian Dam," by Clough, R.W., Chang, K.-T., Chen, H.-Q. and Stephen, R.M., April 1984, (PB84 209 402)A08.

UCB/EERC-84/03 "Refined Modelling of Reinforced Concrete Columns for Seismic Analysis," by Kaba, S.A. and Mahin, S.A., April 1984, (PB84 234 384)A06.

UCB/EERC-84/04 "A New Floor Response Spectrum Method for Seismic Analysis of Multiply Supported Secondary Systems," by Asfura, A. and Der Kiureghian, A., June 1984, (PB84 239 417)A06.

UCB/EERC-84/05 "Earthquake Simulation Tests and Associated Studies of a 1/5th-scale Model of a 7-Story R/C Frame-Wall Test Structure," by Bertero, V.V., Aktan, A.E., Charney, F.A. and Sause, R., June 1984, (PB84 239 409)A09.

UCB/EERC-84/06 "R/C Structural Walls: Seismic Design for Shear," by Aktan, A.E. and Bertero, V.V., 1984.

UCB/EERC-84/07 "Behavior of Interior and Exterior Flat-Plate Connections subjected to Inelastic Load Reversals," by Zee, H.L. and Moehle, J.P., August 1984, (PB86 117 629/AS)A07.

UCB/EERC-84/08 "Experimental Study of the Seismic Behavior of a Two-Story Flat-Plate Structure," by Moehle, J.P. and Diebold, J.W., August 1984, (PB86 122 553/AS)A12.

UCB/EERC-84/09 "Phenomenological Modeling of Steel Braces under Cyclic Loading," by Ikeda, K., Mahin, S.A. and Dermitzakis, S.N., May 1984, (PB86 132 198/AS)A08.

UCB/EERC-84/10 "Earthquake Analysis and Response of Concrete Gravity Dams," by Fenves, G. and Chopra, A.K., August 1984, (PB85 193 902/AS)A11.

UCB/EERC-84/11 "EAGD-84: A Computer Program for Earthquake Analysis of Concrete Gravity Dams," by Fenves, G. and Chopra, A.K., August 1984, (PB85 193 613/AS)A05.

UCB/EERC-84/12 "A Refined Physical Theory Model for Predicting the Seismic Behavior of Braced Steel Frames," by Ikeda, K. and Mahin, S.A., July 1984, (PB85 191 450/AS)A09.

UCB/EERC-84/13 "Earthquake Engineering Research at Berkeley - 1984," by , August 1984, (PB85 197 341/AS)A10.

UCB/EERC-84/14 "Moduli and Damping Factors for Dynamic Analyses of Cohesionless Soils," by Seed, H.B., Wong, R.T., Idriss, I.M. and Tokimatsu, K., September 1984, (PB85 191 468/AS)A04.

UCB/EERC-84/15 "The Influence of SPT Procedures in Soil Liquefaction Resistance Evaluations," by Seed, H.B., Tokimatsu, K., Harder, L.F. and Chung, R.M., October 1984, (PB85 191 732/AS)A04.

UCB/EERC-84/16 "Simplified Procedures for the Evaluation of Settlements in Sands Due to Earthquake Shaking," by Tokimatsu, K. and Seed, H.B., October 1984, (PB85 197 887/AS)A03.

UCB/EERC-84/17 "Evaluation of Energy Absorption Characteristics of Bridges under Seismic Conditions," by Imbsen, R.A. and Penzien, J., November 1984.

UCB/EERC-84/18 "Structure-Foundation Interactions under Dynamic Loads," by Liu, W.D. and Penzien, J., November 1984, (PB87 124 889/AS)A11.

UCB/EERC-84/19 "Seismic Modelling of Deep Foundations," by Chen, C.-H. and Penzien, J., November 1984, (PB87 124 798/AS)A07.

UCB/EERC-84/20 "Dynamic Response Behavior of Quan Shui Dam," by Clough, R.W., Chang, K.-T., Chen, H.-Q., Stephen, R.M., Ghanaat, Y. and Qi, J.-H., November 1984, (PB86 115177/AS)A07.

UCB/EERC-85/01 "Simplified Methods of Analysis for Earthquake Resistant Design of Buildings," by Cruz, E.F. and Chopra, A.K., February 1985, (PB86 112299/AS)A12.

UCB/EERC-85/02 "Estimation of Seismic Wave Coherency and Rupture Velocity using the SMART 1 Strong-Motion Array Recordings," by Abrahamson, N.A., March 1985, (PB86 214 343)A07.

UCB/EERC-85/03 "Dynamic Properties of a Thirty Story Condominium Tower Building," by Stephen, R.M., Wilson, E.L. and Stander, N., April 1985, (PB86 118965/AS)A06.

UCB/EERC-85/04 "Development of Substructuring Techniques for On-Line Computer Controlled Seismic Performance Testing," by Dermitzakis, S. and Mahin, S., February 1985, (PB86 132941/AS)A08.

UCB/EERC-85/05 "A Simple Model for Reinforcing Bar Anchorages under Cyclic Excitations," by Filippou, F.C., March 1985, (PB86 112 919/AS)A05.

UCB/EERC-85/06 "Racking Behavior of Wood-framed Gypsum Panels under Dynamic Load," by Oliva, M.G., June 1985.

UCB/EERC-85/07 "Earthquake Analysis and Response of Concrete Arch Dams," by Fok, K.-L. and Chopra, A.K., June 1985, (PB86 139672/AS)A10.

UCB/EERC-85/08 "Effect of Inelastic Behavior on the Analysis and Design of Earthquake Resistant Structures," by Lin, J.P. and Mahin, S.A., June 1985, (PB86 135340/AS)A08.

UCB/EERC-85/09 "Earthquake Simulator Testing of a Base-Isolated Bridge Deck," by Kelly, J.M., Buckle, I.G. and Tsai, H.-C., January 1986, (PB87 124 152/AS)A06.

UCB/EERC-85/10 "Simplified Analysis for Earthquake Resistant Design of Concrete Gravity Dams," by Fenves, G. and Chopra, A.K., June 1986, (PB87 124 160/AS)A08.

UCB/EERC-85/11 "Dynamic Interaction Effects in Arch Dams," by Clough, R.W., Chang, K.-T., Chen, H.-Q. and Ghanaat, Y., October 1985, (PB86 135027/AS)A05.

UCB/EERC-85/12 "Dynamic Response of Long Valley Dam in the Mammoth Lake Earthquake Series of May 25-27, 1980," by Lai, S. and Seed, H.B., November 1985, (PB86 142304/AS)A05.

UCB/EERC-85/13 "A Methodology for Computer-Aided Design of Earthquake-Resistant Steel Structures," by Austin, M.A., Pister, K.S. and Mahin, S.A., December 1985, (PB86 159480/AS)A10 .

UCB/EERC-85/14 "Response of Tension-Leg Platforms to Vertical Seismic Excitations," by Liou, G.-S., Penzien, J. and Yeung, R.W., December 1985, (PB87 124 871/AS)A08.

UCB/EERC-85/15 "Cyclic Loading Tests of Masonry Single Piers: Volume 4 - Additional Tests with Height to Width Ratio of 1," by Sveinsson, B., McNiven, H.D. and Sucuoglu, H., December 1985.

UCB/EERC-85/16 "An Experimental Program for Studying the Dynamic Response of a Steel Frame with a Variety of Infill Partitions," by Yanev, B. and McNiven, H.D., December 1985.

UCB/EERC-86/01 "A Study of Seismically Resistant Eccentrically Braced Steel Frame Systems," by Kasai, K. and Popov, E.P., January 1986, (PB87 124 178/AS)A14.

UCB/EERC-86/02 "Design Problems in Soil Liquefaction," by Seed, H.B., February 1986, (PB87 124 186/AS)A03.

UCB/EERC-86/03 "Implications of Recent Earthquakes and Research on Earthquake-Resistant Design and Construction of Buildings," by Bertero, V.V., March 1986, (PB87 124 194/AS)A05.

UCB/EERC-86/04 "The Use of Load Dependent Vectors for Dynamic and Earthquake Analyses," by Leger, P., Wilson, E.L. and Clough, R.W., March 1986, (PB87 124 202/AS)A12.

UCB/EERC-86/05 "Two Beam-To-Column Web Connections," by Tsai, K.-C. and Popov, E.P., April 1986, (PB87 124 301/AS)A04.

UCB/EERC-86/06 "Determination of Penetration Resistance for Coarse-Grained Soils using the Becker Hammer Drill," by Harder, L.F. and Seed, H.B., May 1986, (PB87 124 210/AS)A07.

UCB/EERC-86/07 "A Mathematical Model for Predicting the Nonlinear Response of Unreinforced Masonry Walls to In-Plane Earthquake Excitations," by Mengi, Y. and McNiven, H.D., May 1986, (PB87 124 780/AS)A06.

UCB/EERC-86/08 "The 19 September 1985 Mexico Earthquake: Building Behavior," by Bertero, V.V., July 1986.

UCB/EERC-86/09 "EACD-3D: A Computer Program for Three-Dimensional Earthquake Analysis of Concrete Dams," by Fok, K.-L., Hall, J.F. and Chopra, A.K., July 1986, (PB87 124 228/AS)A08.

UCB/EERC-86/10 "Earthquake Simulation Tests and Associated Studies of a 0.3-Scale Model of a Six-Story Concentrically Braced Steel Structure," by Uang, C.-M. and Bertero, V.V., December 1986, (PB87 163 564/AS)A17.

UCB/EERC-86/11 "Mechanical Characteristics of Base Isolation Bearings for a Bridge Deck Model Test," by Kelly, J.M., Buckle, I.G. and Koh, C.-G., November 1987.

UCB/EERC-86/12 "Effects of Axial Load on Elastomeric Isolation Bearings," by Koh, C.-G. and Kelly, J.M., 1987.

UCB/EERC-87/01 "The FPS Earthquake Resisting System: Experimental Report," by Zayas, V.A., Low, S.S. and Mahin, S.A., June 1987.

UCB/EERC-87/02 "Earthquake Simulator Tests and Associated Studies of a 0.3-Scale Model of a Six-Story Eccentrically Braced Steel Structure," by Whittaker, A., Uang, C.-M. and Bertero, V.V., July 1987.

UCB/EERC-87/03 "A Displacement Control and Uplift Restraint Device for Base-Isolated Structures," by Kelly, J.M., Griffith, M.C. and Aiken, I.D., April 1987.

UCB/EERC-87/04 "Earthquake Simulator Testing of a Combined Sliding Bearing and Rubber Bearing Isolation System," by Kelly, J.M. and Chalhoub, M.S., 1987.

UCB/EERC-87/05 "Three-Dimensional Inelastic Analysis of Reinforced Concrete Frame-Wall Structures," by Moazzami, S. and Bertero, V.V., May 1987.

UCB/EERC-87/06 "Experiments on Eccentrically Braced Frames with Composite Floors," by Ricles, J. and Popov, E., June 1987.

UCB/EERC-87/07 "Dynamic Analysis of Seismically Resistant Eccentrically Braced Frames," by Ricles, J. and Popov, E., June 1987.

UCB/EERC-87/08 "Undrained Cyclic Triaxial Testing of Gravels-The Effect of Membrane Compliance," by Evans, M.D. and Seed, H.B., July 1987.

UCB/EERC-87/09 "Hybrid Solution Techniques for Generalized Pseudo-Dynamic Testing," by Thewalt, C. and Mahin, S.A., July 1987.

UCB/EERC-87/10 "Ultimate Behavior of Butt Welded Splices in Heavy Rolled Steel Sections," by Bruneau, M. Mahin, S.A. and Popov, E., September 1987.

UCB/EERC-87/11 "Residual Strength of Sand from Dam Failures in the Chilean Earthquake of March 3, 1985," by De Alba, P., Seed, H.B., Retamal, E. and Seed, R.B., September 1987.

UCB/EERC-87/12 "Inelastic Seismic Response of Structures with Mass or Stiffness Eccentricities in Plan," by Bruneau, M. and Mahin, S.A., September 1987.

UCB/EERC-87/13 "CSTRUCT: An Interactive Computer Environment for the Design and Analysis of Earthquake Resistant Steel Structures," by Austin, M.A., Mahin, S.A. and Pister, K.S., September 1987.

UCB/EERC-87/14 "Experimental Study of Reinforced Concrete Columns Subjected to Multi-Axial Loading," by Low, S.S. and Moehle, J.P., September 1987.

UCB/EERC-87/15 "Relationships between Soil Conditions and Earthquake Ground Motions in Mexico City in the Earthquake of Sept. 19, 1985," by Seed, H.B., Romo, M.P., Sun, J., Jaime, A. and Lysmer, J., October 1987.

UCB/EERC-87/16 "Experimental Study of Seismic Response of R. C. Setback Buildings," by Shahrooz, B.M. and Moehle, J.P., October 1987.

UCB/EERC-87/17 "The Effect of Slabs on the Flexural Behavior of Beams," by Pantazopoulou, S.J. and Moehle, J.P., October 1987.

UCB/EERC-87/18 "Design Procedure for R-FBI Bearings," by Mostaghel, N. and Kelly, J.M., November 1987.

UCB/EERC-87/19 "Analytical Models for Predicting the Lateral Response of R C Shear Walls: Evaluation of their Reliability," by Vulcano, A. and Bertero, V.V., November 1987.

UCB/EERC-87/20 "Earthquake Response of Torsionally-Coupled Buildings," by Hejal, R. and Chopra, A.K., December 1987.

UCB/EERC-87/21 "Dynamic Reservoir Interaction with Monticello Dam," by Clough, R.W., Ghanaat, Y. and Qiu, X-F., December 1987.

UCB/EERC-87/22 "Strength Evaluation of Coarse-Grained Soils," by Siddiqi, F.H., Seed, R.B., Chan, C.K., Seed, H.B. and Pyke, R.M., December 1987.

UCB/EERC-88/01 "Seismic Behavior of Concentrically Braced Steel Frames," by Khatib, I., Mahin, S.A. and Pister, K.S., January 1988.

UCB/EERC-88/02 "Experimental Evaluation of Seismic Isolation of Medium-Rise Structures Subject to Uplift," by Griffith, M.C., Kelly, J.M., Coveney, V.A. and Koh, C.G., January 1988.

UCB/EERC-88/03 "Cyclic Behavior of Steel Double Angle Connections," by Astaneh-Asl, A. and Nader, M.N., January 1988.

UCB/EERC-88/04 "Re-evaluation of the Slide in the Lower San Fernando Dam in the Earthquake of Feb. 9, 1971," by Seed, H.B., Seed, R.B., Harder, L.F. and Jong, H.-L., April 1988.

UCB/EERC-88/05 "Experimental Evaluation of Seismic Isolation of a Nine-Story Braced Steel Frame Subject to Uplift," by Griffith, M.C., Kelly, J.M. and Aiken, I.D., May 1988.

UCB/EERC-88/06 "DRAIN-2DX User Guide.," by Allahabadi, R. and Powell, G.H., March 1988.

UCB/EERC-88/07 "Cylindrical Fluid Containers in Base-Isolated Structures," by Chalhoub, M.S. and Kelly, J.M., April 1988.

UCB/EERC-88/08 "Analysis of Near-Source Waves: Separation of Wave Types using Strong Motion Array Recordings," by Darragh, R.B., June 1988.

UCB/EERC-88/09 "Alternatives to Standard Mode Superposition for Analysis of Non-Classically Damped Systems," by Kusainov, A.A. and Clough, R.W., June 1988.

UCB/EERC-88/10 "The Landslide at the Port of Nice on October 16, 1979," by Seed, H.B., Seed, R.B., Schlosser, F., Blondeau, F. and Juran, I., June 1988.

UCB/EERC-88/11 "Liquefaction Potential of Sand Deposits Under Low Levels of Excitation," by Carter, D.P. and Seed, H.B., August 1988.

UCB/EERC-88/12 "Nonlinear Analysis of Reinforced Concrete Frames Under Cyclic Load Reversals," by Filippou, F.C. and Issa, A., September 1988.

UCB/EERC-88/13 "Implications of Recorded Earthquake Ground Motions on Seismic Design of Building Structures," by Uang, C.-M. and Bertero, V.V., September 1988.

UCB/EERC-88/14 "An Experimental Study of the Behavior of Dual Steel Systems," by Whittaker, A.S., Uang, C.-M. and Bertero, V.V., September 1988.

UCB/EERC-88/15 "Dynamic Moduli and Damping Ratios for Cohesive Soils," by Sun, J.I., Golesorkhi, R. and Seed, H.B., August 1988.

UCB/EERC-88/16 "Reinforced Concrete Flat Plates Under Lateral Load: An Experimental Study Including Biaxial Effects," by Pan, A. and Moehle, J., November 1988.

UCB/EERC-88/17 "Earthquake Engineering Research at Berkeley - 1988," November 1988.

UCB/EERC-88/18 "Use of Energy as a Design Criterion in Earthquake-Resistant Design," by Uang, C.-M. and Bertero, V.V., November 1988.

UCB/EERC-88/19 "Steel Beam-Column Joints in Seismic Moment Resisting Frames," by Tsai, K.-C. and Popov, E.P., September 1988.

UCB/EERC-88/20 "Base Isolation in Japan, 1988," by Kelly, J.M., December 1988.

UCB/EERC-89/01 "Behavior of Long Links in Eccentrically Braced Frames," by Engelhardt, M.D. and Popov, E.P., January 1989.

UCB/EERC-89/02 "Earthquake Simulator Testing of Steel Plate Added Damping and Stiffness Elements," by Whittaker, A., Bertero, V.V., Alonso, J. and Thompson, C., January 1989.

UCB/EERC-89/03 "Implications of Site Effects in the Mexico City Earthquake of Sept. 19, 1985 for Earthquake-Resistant Design Criteria in the San Francisco Bay Area of California," by Seed, H.B. and Sun, J.I., March 1989.